

1 **Title:**

2 Modelling the role of fires in the terrestrial carbon balance by incorporating SPITFIRE into the
3 global vegetation model ORCHIDEE – Part 2: carbon emissions and the role of fires in the global
4 carbon balance

5

6 **Running title:** Modelling the role of fires in the global carbon balance

7

8 C. Yue^{1,2}, P. Ciais², P. Cadule², K. Thonicke³, T. T. van Leeuwen^{4,5}

9

10 ¹Laboratoire de Glaciologie et Géophysique de l'Environnement, UJF, CNRS, Saint Martin
11 d'Hères CEDEX, France

12 ²Laboratoire des Sciences du Climat et de l'Environnement, LSCE CEA CNRS UVSQ, 91191 Gif-
13 Sur-Yvette, France

14 ³Potsdam Institute for Climate Impact Research (PIK) e.V., Telegraphenberg A31, 14473
15 Potsdam, Germany

16 ⁴SRON Netherlands Institute for Space Research, Sorbonnelaan 2, 3584 CA, Utrecht, The
17 Netherlands

18 ⁵Institute for Marine and Atmospheric Research Utrecht, Utrecht University, Princetonplein 5,
19 3584 CC, Utrecht, The Netherlands

20

21 corresponding author: Chao Yue, chao.yue@lsce.ipsl.fr

22

23 **Abstract**

24 Carbon dioxide emissions from wild and anthropogenic fires return the carbon absorbed by plants
25 to the atmosphere, and decrease the sequestration of carbon by land ecosystems. Future climate
26 warming will likely increase the frequency of fire-triggering drought, so that the future terrestrial
27 carbon uptake will depend on how fires respond to altered climate variation. In this study, we
28 modelled the role of fires in the global terrestrial carbon balance for 1901–2012, using the global
29 vegetation model ORCHIDEE equipped with the SPITFIRE model. We conducted two
30 simulations with and without the fire module being activated, using a static land cover. The
31 simulated global fire carbon emissions for 1997–2009 are 2.1 Pg C yr⁻¹, which is close to the 2.0
32 Pg C yr⁻¹ as estimated by GFED3.1. The simulated land carbon uptake after accounting for
33 emissions for 2003–2012 is 3.1 Pg C yr⁻¹, which is within the uncertainty of the residual carbon
34 sink estimation (2.8 +/- 0.8 Pg C yr⁻¹). Fires are found to reduce the terrestrial carbon uptake by
35 0.32 Pg C yr⁻¹ over 1901–2012, or 20% of the total carbon sink in a world without fire. The fire-
36 induced land sink reduction (SR_{fire}) is significantly correlated with climate variability, with larger
37 sink reduction occurring in warm and dry years, in particular during El Niño events. Our results

1 suggest a "fire respiration partial compensation". During the ten lowest SR_{fire} years ($SR_{\text{fire}} = 0.17$
2 Pg C yr^{-1}), fires mainly compensate for the heterotrophic respiration that would occur in a world
3 without fire. By contrast, during the ten highest SR_{fire} fire years ($SR_{\text{fire}} = 0.49 \text{ Pg C yr}^{-1}$), fire
4 emissions exceed far their "respiration partial compensation" and create a larger reduction in
5 terrestrial carbon uptake. Our findings have important implications for the future role of fires in
6 the terrestrial carbon balance, because the capacity of terrestrial ecosystems to sequester carbon
7 will be diminished by future climate change characterized by increased frequency of droughts and
8 extreme El Niño events.

9 **1 Introduction**

10 Vegetation fires contribute significantly to the interannual variability (IAV) of atmospheric
11 CO_2 concentration. Deforestation and peat fires emit carbon that is not offset by rapid vegetation
12 regrowth, and thus contribute to a net increase of atmospheric CO_2 (Bowman et al., 2009;
13 Langenfelds et al., 2002; Schimel and Baker, 2002; van der Werf et al., 2009). Besides the direct
14 effect of fires in reducing the capacity of terrestrial ecosystems to sequester carbon, other
15 greenhouse gases (e.g., CH_4 , N_2O), ozone precursors, and aerosols emitted by fires are a net
16 source of radiative forcing (Podgorny et al., 2003; Tosca et al., 2010; Ward et al., 2012). Finally,
17 fires can also impact climate by changing the land surface properties, such as vegetation structure
18 and albedo (Beck et al., 2011; Jin et al., 2012), as well as the energy partitioning (Liu and
19 Randerson, 2008; Rocha and Shaver, 2011). Changes in temperature and precipitation patterns, in
20 particular drought frequency and severity, also influence fire regimes and their emissions (Balshi
21 et al., 2009; Kloster et al., 2012; Westerling et al., 2011) causing complex fire-vegetation-climate
22 interactions.

23 The estimation of global carbon emissions from fires was pioneered by Seiler and Crutzen
24 (1980), who used available literature data of field experiments to assess important fire parameters
25 like area burned, fuel load and the combustion completeness. More recently, large-scale spatially
26 explicit estimation of fire carbon emissions has been aided by satellite-derived burned area and
27 active fire counts (Giglio et al., 2010; Roy et al., 2008; Tansey et al., 2008), as well as vegetation
28 models in which burned area is either prescribed (Randerson et al., 2012; van der Werf et al.,
29 2006, 2010) or simulated with a prognostic fire model (Kloster et al., 2010; Li et al., 2013;
30 Prentice et al., 2011; Thonicke et al., 2010). Several recent estimates have converged to give
31 annual fire carbon emissions of $\sim 2 \text{ Pg C yr}^{-1}$, as pointed out by Li et al. (2014). Van der Werf et al.
32 (2006) showed that the IAV of global fire carbon emissions is decoupled from the variation in
33 burned area, mainly due to the disproportionate contribution to global emissions by fires with a
34 large fuel consumption (forest fire, deforestation fire and peat fire). Prentice et al. (2011)
35 examined how burned area in tropical and subtropical regions is influenced by the El Niño
36 Southern Oscillation (ENSO) climate variability, and quantified the contribution of fire emission
37 anomaly to the anomaly of land sink as diagnosed by atmospheric inversions. However, it is only

1 recently that Li et al. (2014) have simultaneously constrained the simulated fire carbon emissions
2 and net biome production (NBP, i.e., the land carbon sink) in their absolute terms, employing a
3 modelling approach. These modelled components of the carbon balance have rarely been reported
4 simultaneously before. Li et al. (2014) also compared the difference in simulated NBP from two
5 simulations with and without fires. However, the specific climatic driving factors for this fire-
6 induced NBP difference have not been investigated. Given the profound perturbation of the
7 climate system by human activities (Cai et al., 2014; Liu et al., 2013; Prudhomme et al., 2013) and
8 with fire activities likely increase in the future (Flannigan et al., 2009; Kloster et al., 2012), it is
9 therefore important to examine how fires and their contribution to the global carbon balance have
10 responded to historical climate variations. This knowledge will give us insight into the likely
11 impact of fires on the future land carbon balance.

12 Just as vegetation can be classified into biomes according to its climatic, morphological and
13 physiological features, so fires occurring under different climate and vegetation patterns have
14 distinctive features that allow them to be characterized by *fire regime*. Attributes of different fire
15 regimes include the frequency, season, size, intensity and extent of fires (Gill and Allan, 2008).
16 Trade-offs may exist between these different aspects of fire, e.g., ecosystems with frequent fires
17 often have a long fire season but can hardly support high-intensity fires because of their low fuel
18 load (Saito et al., 2014). Efforts have been made to further classify fires by examining co-
19 occurring fire characteristics and relating these fire groups (named *pyromes*) to climatic, human
20 and economic factors (Archibald et al., 2013; Chuvieco et al., 2008). Archibald et al. (2013)
21 proposed an approach to divide fires into five pyromes, using the most extensive available global
22 fire regime datasets including fire extent, fire season length, fire return interval, fire size and fire
23 intensity. Though related to the biome distribution, pyromes are different from biomes. For
24 example, the "Intermediate–Cool–Small" fire pyrome occurs throughout the globe, particular in
25 regions of deforestation and agriculture, whereas the "Frequent–Intense–Large" fire pyrome is
26 associated with tropical grassland-dominated systems. Different fire pyromes are suspected to also
27 have impacts on the amount, seasonality and IAV of fire carbon emissions, and further
28 consequences on the terrestrial carbon balance.

29 In a companion study (Yue et al., 2014), we incorporated the prognostic fire model
30 SPITFIRE into the global vegetation model ORCHIDEE, and evaluated the modelled burned area
31 and fire regimes during the 20th century using multiple observation datasets. In the present study,
32 fire carbon emissions are simulated for 1901–2012, and the role of fires in the terrestrial carbon
33 balance is investigated in relation to different climatic drivers and fire pyromes. Here we address
34 what difference fires have made in the global terrestrial carbon balance, and how this difference is
35 driven by large-scale climate variations, with a special focus on the naturally occurring vegetation
36 fires. More specifically, the objectives of this study are to: (a) Benchmark the ORCHIDEE-
37 SPITFIRE model in terms of simulated carbon emissions against GFED3.1 data, and identify
38 model strengths and weaknesses. (b) Investigate the role of fires in the terrestrial carbon balance

1 for 1901–2012 and the climatic factors driving its magnitude and temporal variation. This
2 objective is tackled by conducting two simulations with and without fire occurrence. (c) Examine
3 the characteristics of different fire regimes (as defined in Archibald et al., 2013) in terms of the
4 role of fires in the terrestrial carbon balance. We hypothesize that more frequent and larger fires
5 will have greater carbon consumption rates than infrequent and smaller ones, and consequently,
6 the fire-induced carbon uptake reduction is larger in the former type of fires.

7 **2 Data and methods**

8 2.1 ORCHIDEE land surface model

9 ORCHIDEE is a global dynamic vegetation model that simulates the exchange of energy,
10 water and carbon between the atmosphere and the land surface. It is the land surface model of the
11 Earth system model IPSL-CM5 (Dufresne et al., 2013; Krinner et al., 2005). The processes and
12 equations of the SPITFIRE fire model (Thonicke et al., 2010) were implemented in ORCHIDEE,
13 with some modifications being described in Yue et al. (2014). There, the model was evaluated
14 against different satellite observations for simulated burned areas and fire regimes.

15 The SPITFIRE module simulates burned area and fire consequences (e.g., emissions, plant
16 mortality) in a mostly mechanistic way. The central underlying engine is the Rothermel's fire
17 spread model (Rothermel, 1972; Pyne et al., 1996; Wilson, 1982), which links fire spread rate to
18 fuel state, weather conditions and fire physics. Weather and fuel moisture conditions determine the
19 time that a fire persists, which, combined with fire spread rate, yield an estimate of mean fire size.
20 Ignition sources are scaled into fire numbers depending on weather conditions, with sources from
21 both lightning and human activities being included. The daily burned area is thus derived as the
22 product of fire number and mean fire size. Anthropogenic ignitions are estimated as a function of
23 population density with the maximum ignition being obtained at ca. 16 ind km⁻² (Venevsky et al.
24 2002, Thonicke et al. 2010). Anthropogenic ignitions are implicitly suppressed by human within
25 the ignition equation, while lightning ignitions are not suppressed.

26 Fire carbon emissions follow a classical paradigm (Seiler and Crutzen, 1980) as the product
27 of daily burned area, fuel load, and combustion completeness. Dead litter on the ground and live
28 biomass from grasses and trees are available for burning. For live grass biomass and dead litter,
29 combustion completeness is calculated as a function of fuel moisture state following the approach
30 of Peterson and Ryan (1986). Tree crown live biomass consumption is simulated to depend on fire
31 intensity and fire scorching height. Two factors are considered concerning fire-caused tree
32 mortality: damage to tree crown because of crown scorching; and cambial damage linked with fire
33 persistence time and tree bark resistance to fire. We refer the reader to Yue et al. (2014) and
34 Thonicke et al. (2010) for a more detailed description of the fire module.

35 The simulation of combustion completeness (CC) for surface dead fuel was modified
36 compared to the original scheme as presented by Thonicke et al. (2010). In SPITFIRE, the

1 calculation of surface fuel CC follow Peterson and Ryan (1986), which allow CC to increase with
2 decreasing fuel wetness and level out when the fuel wetness drops below some threshold (see Fig.
3 1 in Yue et al., 2014). During the model testing, it was found that simulated CCs were much
4 higher than the recently compiled field observations for different biomes (van Leeuwen et al.,
5 2014). We thus adjusted the maximum CC for fuel classes of 100 (with original maximum CC as
6 1.0) and 1000h (with original maximum CC as 0.8) to mean values provided by an earlier version
7 of van Leeuwen et al. (2014) (Detmers, personal communication) which was available when
8 preparing the current study. The categorization of fuels in terms of magnitude of hours describes
9 the order of magnitude of time required to lose (or gain) 63% of the fuel moisture difference with
10 the equilibrium moisture state under defined atmospheric conditions (Thonicke et al., 2010). The
11 mean observational values were adopted as the maximum values in the model equations, because
12 the simulated burned area is dominated with low fuel wetness, so that the simulated CC value is
13 close to its maximum. However, we kept the original CC simulation scheme in the original
14 SPITFIRE model for the convenience of future elaboration. According to the earlier version
15 dataset of van Leeuwen et al. (2014), the biome-dependent maximum CC is 0.49 for tropical
16 broadleaf evergreen and seasonal dry forests, 0.45 for temperate forests, 0.41 for boreal forests,
17 and 0.85 for grasslands.

18 2.2 Model productivity calibration

19 As shown by Yue et al. (2014), the mean annual burned area on non-crop lands for 2001–
20 2006 simulated to be 346 Mha yr⁻¹ by ORCHIDEE. This falls within the range 287–384 Mha yr⁻¹
21 from three global satellite-derived datasets (GLOBCARBON, L3JRC and GFED3.1), and is
22 close to the 344 Mha yr⁻¹ obtained in GFED3.1 when agricultural fires are excluded. The
23 simulated global burned area on decadal time scale during the 20th century agrees moderately
24 well with the historical reconstruction by Mouillot and Field (2005), corrected for regional mean
25 bias using GFED3.1 for 1997–2000. However, one ORCHIDEE model shortcoming is that the
26 terrestrial productivity is overestimated (as also revealed by Piao et al., 2013) possibly due to the
27 absence of nutrient limitation, which leads to overestimated fire carbon emissions.

28 The simulated global gross primary productivity (GPP) by ORCHIDEE (version 1.9.6) as
29 driven by CRUNCEP climate forcing data is 205 Pg C yr⁻¹ for 1982–2010. This is much higher
30 than the estimated 119 +/- 6 Pg C yr⁻¹ by Jung et al. (2011), which was derived by interpolating
31 eddy-covariance measurements over the globe using climate, remote-sensing fAPAR and a
32 multiple tree regression ensemble algorithm (hereafter referred to as MTE-GPP). In order to
33 correct for the positive bias of GPP, we use a simple approach to adjust the optimal carboxylation
34 rates (V_{cmax} , in unit of $\mu\text{mol m}^{-2} \text{s}^{-1}$, see Eq.A2–A6 in Krinner et al., 2005) to match the simulated
35 total GPP with the MTE-GPP reported for different biomes.

36 The default ORCHIDEE plant functional types (PFTs, excluding bare land) were grouped
37 into five biomes: boreal forest, temperate forest, tropical forest, grassland and agricultural land.

1 The spatial extent of each biome was determined as the area where a corresponding ORCHIDEE
2 PFT occupies more than 90% of a grid cell in the 0.5-degree MTE-GPP dataset. A ratio of
3 simulated GPP to MTE-GPP was determined for each biome, and this ratio was used to adjust
4 carboxylation rates (with the maximum potential rate of RuBP regeneration V_{jmax} being set to
5 double of V_{cmax}). The original and calibrated carboxylation rates together with the biome-specific
6 GPP ratios are given in Table S1. We emphasize that the approach employed here is an empirical
7 and simple adjustment to calibrate ORCHIDEE productivity, but does not necessarily result in
8 optimized carboxylation rates that agree with, for example, leaf-scale measurements (e.g., see
9 discussion by Rogers, 2014).

10 2.3 Simulations and input datasets

11 To evaluate the role of fires in the global terrestrial carbon balance, two parallel simulations
12 were conducted: fireON and fireOFF, with SPITFIRE being switched on or off, respectively. In
13 both simulations, the dynamic vegetation module of ORCHIDEE was de-activated, and a current-
14 day vegetation distribution map (converted into the 13-PFT map in ORCHIDEE based on IGBP 1-
15 km vegetation map, http://webmap.ornl.gov/wcsdown/dataset.jsp?ds_id=930) was used as the
16 static land cover. Here, fire-vegetation-climate feedback was not included because the relative
17 fractions of different PFTs remain the same over the simulation period. It means not only that fires
18 associated with land cover change (deforestation fires) are not included, but also that wildfires are
19 not affected by changing PFTs.

20 Agricultural fires are not simulated in the model for two reasons. First, the timing of
21 agricultural burning is strongly constrained by the sowing and harvest date (Magi et al., 2012). An
22 enhanced crop phenology module is under development for ORCHIDEE and this will allow
23 precise agricultural fire seasons to be included in the future. Second, agricultural fires are
24 normally under strict human control and the spread and size of fires are limited by field size; they
25 are thus very different from wildfires and warrant a special modelling approach. Carbon emissions
26 from tropical and boreal peat fires are not explicitly simulated, although the model does simulate
27 some burned fraction in tropical regions where deforestation fires dominate. Because the model
28 could capture the "climate window" when the climate is relatively dry and deforestation fires are
29 possible. Thus even though the model does not explicitly simulate deforestation fires using a land-
30 cover-change approach, it does capture some fire activities in the region dominated by
31 deforestation fires, and simulate them like natural wildfires. Figure S1 compares simulated and
32 GFED3.1 emissions for the tropical region of 20°S–20°N for different types of fire averaged over
33 1997–2009. The simulated fire emissions were partitioned into forest and grassland fires, and the
34 GFED3.1 emissions were partitioned into "deforestation + forest", "woodland + savanna", and
35 "agriculture + peat". The model could capture part of forest and deforestation fire emissions in this
36 region (simulated 0.28 Pg C yr⁻¹ against GFED3.1 0.44 Pg C yr⁻¹, of which deforestation fires
37 account for 0.33 Pg C yr⁻¹ and naturally occurring forest fires 0.11 Pg C yr⁻¹), because simulated

1 total forest fire emissions in this region are larger than those from natural forest fires as given by
2 GFED3.1 data. The simulated emissions are slightly lower than GFED3.1 data, even when
3 emissions from agriculture and peat fires are excluded (simulated 1.38 Pg C yr⁻¹ for forest +
4 grassland; against GFED3.1 1.50 Pg C yr⁻¹ for deforestation + forest + woodland + savanna, and
5 1.63 Pg C yr⁻¹ when agriculture and peat are further included). This shows that the model has
6 limited capability in capturing fire emissions in tropical regions.

7 Both fireON and fireOFF simulations followed the same protocol, which comprised three
8 steps. For both simulations, the model was first run for 200 years (including a 3000-year soil-only
9 spin-up to speed up the equilibrium of slow and passive soil carbon pools) starting from bare
10 ground without fire, with atmospheric CO₂ being fixed at the pre-industrial level (285 ppm) and
11 climate data of 1901–1930 being cycled. For the fireON simulation, after this first spin-up, the
12 model was run for a second spin-up of 150 years with the fire model being switched on, to allow
13 carbon stocks to reach an equilibrium state under pre-industrial fire disturbance. For this second
14 spin-up with fires, atmospheric CO₂ was set at pre-industrial level and climate data of 1901–1930
15 were cycled. We verify that during last 50 years of this second spin-up, the mineral soil carbon
16 stock (i.e., the sum of active, slow and passive soil carbon pools in the model) varies within 0.1%
17 and no significant trend exists for simulated global total carbon balance. This simulation was
18 followed by a third transient simulation for 1850–2012, with variable climate, atmospheric CO₂
19 and population density data.

20 The fireOFF simulation follows the same first spin-up, second spin-up and transient steps as
21 the fireON simulation, except that the fire model is switched off throughout all simulations. The
22 climate data used for 1901–2012 are 6-hourly CRUNCEP data
23 (http://dods.extra.cea.fr/store/p529viov/cruncep/V4_1901_2012/readme.htm). During the period
24 1850–1900 when CRUNCEP climate data were not available, the data of 1901–1910 were used
25 and cycled. Lightning data were retrieved from the High Resolution Monthly Climatology of
26 lightning flashes by the Lightning Imaging Sensor–Optical Transient Detector (LIS/OTD)
27 (http://gcmd.nasa.gov/records/GCMD_lohrmc.html). The LIS/OTD dataset provides mean
28 monthly flash rates over the period of 1995–2000 on a 0.5° grid, which were cycled each year
29 throughout the simulation. The annual historical population density data were retrieved from the
30 Netherlands Environmental Assessment Agency
31 (<http://themasites.pbl.nl/tridion/en/themasites/hyde/download/index-2.html>). Please refer to Yue et
32 al. (2014) for the detailed information on these input datasets.

33 For the fireON simulation, after the second spin-up, there is a global carbon sink of 0.19 Pg
34 C yr⁻¹ over the last 50 years prior to the transient simulation due to the not-fully complete
35 equilibrium of slow soil carbon pools. We verified that this sink has a negligible trend (annual
36 trend of 0.003 Pg C yr⁻¹). For the fireOFF simulation, the residual sink before the transient
37 simulation is 0.17 Pg C yr⁻¹ (with a negligible annual trend of -0.001 Pg C yr⁻¹). Because the
38 ORCHIDEE version used here is computationally expensive, we did not run the model until a

1 complete carbon saturation state. The simulated annual global total net biome production (NBP)
2 during 1901–2012 was bias-corrected for this incomplete spin-up by subtracting the remaining
3 positive NBP over the last 50 years of the second spin-up. No spatial corrections were made.

4 2.4 Land-atmosphere carbon flux conventions

5 We define NEP, the net ecosystem production, as:

$$6 \quad \text{NEP} = \text{NPP} - \text{RH} - \text{CH} \quad (1)$$

7 where NPP is net primary production, RH is the heterotrophic respiration, and CH is the harvested
8 crop yield. We assume that crop harvest is released into the atmosphere within the year when
9 being harvested. Next, we define NBP, the net biome production as:

$$10 \quad \text{NBP} = \text{NEP} - \text{FE} \quad (2)$$

11 where FE is fire carbon emission. In case of fireOFF simulation, fire carbon emissions would be
12 zero. If we do not include other components of the carbon balance term (e.g., herbivore
13 consumption, biogenic volatile organic compound emissions, lateral carbon transfer by rivers and
14 erosion), NBP is here considered as land carbon sink. We expect that fires reduce this carbon sink,
15 and define the "fire-induced sink reduction" as:

$$16 \quad \text{SR}_{\text{fire}} = \text{NBP}_{\text{OFF}} - \text{NBP}_{\text{ON}} \quad (3)$$

17 where NBP_{OFF} is NBP by fireOFF simulation and NBP_{ON} is NBP by fireON simulation. We
18 further define a term "sink efficiency (SE)" as NBP divided by NPP, which describes the fraction
19 of NPP used to sequester carbon from the atmosphere.

20 2.5 Evaluation datasets and other datasets

21 The GFED3.1 fire carbon emissions from the CASA biosphere model forced by GFED3.1
22 burned area data were used to evaluate simulated fire carbon emissions (van der Werf et al., 2010).
23 Much work has been done to calibrate the CASA model against observations, e.g., in terms of
24 productivity and NPP allocation (van der Werf et al., 2006; 2010). Carbon emissions from six
25 different fire types are identified in GFED3.1 data, namely forest fire, grassland fire, woodland
26 fire, agricultural fire, deforestation and peatland fires. For the convenience of description,
27 emission sources of the former three types of fire are tentatively referred to as natural sources (that
28 ORCHIDEE-SPITFIRE simulates explicitly), and those of the latter three types as anthropogenic
29 sources (that ORCHIDEE does not explicitly include, although it is able to capture part of the
30 deforestation fire emissions as explained in Sect. 2.3). Note that the grouping of different emission
31 sources in GFED3.1 data does not necessarily reflect the exact nature of different fire types. For
32 example, peat fires in tropics are mainly due to intentional drainage followed by burning to
33 remove a (logged) forest (thus anthropogenic, e.g., Marlier et al., 2015), while in northern high-
34 latitude regions peatland fires might be due to drought (thus natural, e.g. Turetsky et al., 2011).

35 Not all anthropogenic carbon emissions (mainly from fossil fuel consumption, cement

1 production and deforestation) into the atmosphere remain there, and part of them are absorbed by
2 the terrestrial ecosystem (land sink) and the ocean (ocean sink). The so-called residual carbon sink
3 in land ecosystems can be obtained by subtracting the annual CO₂ accumulation in the atmosphere
4 and the ocean sink from the total anthropogenic carbon emissions (Le Quéré et al., 2013). This
5 residual sink was used here to be compared with simulated carbon sink.

6 The fire variability at global and regional scales is known to relate to the ENSO mode of
7 climate variability (Kitzberger et al., 2001; Prentice et al., 2011; van der Werf et al., 2004), mainly
8 affecting the tropics but with global teleconnections (Kiladis and Diaz, 1989). The Southern
9 Oscillation Index (SOI, <http://www.bom.gov.au/climate/current/soihtml1.shtml>) is an indicator of
10 the development and intensity of El Niño or La Niña events in the Pacific Ocean (negative values
11 of the SOI below -8 often indicate El Niño episodes and the reverse La Niña episodes). SOI was
12 used here to investigate the fire-induced sink reduction in relation to this large-scale climate
13 oscillation.

14 Finally, the fire pyrome distribution map of Archibald et al. (2013) was used to relate the
15 influence of fires on NBP to different fire pyromes (Fig. S2). Five fire pyromes were identified by
16 using a Bayesian clustering algorithm with information on key characteristics of fire regimes –
17 size, frequency, intensity, season and extent. The five pyromes are: FIL (Frequent–Intense–Large);
18 FCS (Frequent–Cool–Small); RIL (Rare–Intense–Large) (RIL); RCS (Rare–Cool–Small) and ICS
19 (Intermediate–Cool–Small). Frequent fires (FIL and FCS) are characterized by large annual
20 burned fractions in areas with a relatively long fire season. Australia has large, intense fires (FIL
21 pyrome), whereas in Africa, smaller less intense fires (FCS pyrome) dominate. Rare fires (RIL and
22 RCS pyromes) are found in areas with a short fire season, dominating in temperate and boreal
23 regions (see Table 1 and Fig. 2 in Archibald et al., 2013 and the descriptions for more
24 information).

25 **3 Results and discussion**

26 3.1 Calibrated productivity and simulated burned area

27 The calibration of carboxylation rates significantly improved the model-observation
28 agreement in terms of the distribution of GPP as a function of annual precipitation (Fig. 1). The
29 calibrated model is also able to capture the productivity decrease when annual precipitation
30 exceeds 3000 mm (Fig. 1). The simulated global GPP for 1982–2010 is 125 Pg C yr⁻¹, close to the
31 119 +/- 6 Pg C yr⁻¹ given by Jung et al. (2011). The simulated global NPP for 2000–2009 is 61 Pg
32 C yr⁻¹, close to the 54 Pg C yr⁻¹ estimated by Zhao and Running (2010) using MODIS satellite
33 data and light-use efficiency conversion factors.

34 The simulated global burned area for 2001–2006 is 239 Mha yr⁻¹, lower than the original
35 346Mha yr⁻¹ before calibration (Yue et al., 2014). This reduction of simulated burned area mainly
36 occurs in the regions with high fire frequency where GPP was decreased by the calibration (Fig.

1 2). After the GPP calibration, the burned fraction of grassland and savanna ecosystems in Africa,
2 Australia and South America, became underestimated compared to GFED3.1 (Fig. 2b and d). The
3 reduction in simulated burned fraction is related to the reduced amount of dead fuel on the surface
4 (Fig. S3) in response to the lower GPP – the latter reduces fire spread rates and fire sizes.

5 3.2 Temporal and spatial patterns of global fire carbon emissions

6 3.2.1 Comparison of simulated carbon emissions with GFED3.1 at the global scale

7 The simulated mean annual global fire carbon emissions for 1997–2009 are 2.1 Pg C yr^{-1} ,
8 close to the estimate of 2.0 Pg C yr^{-1} by GFED3.1 data, where emissions from both natural and
9 anthropogenic sources are included (Fig. 3), and higher than the 1.5 Pg C yr^{-1} when peat,
10 deforestation and agricultural fires are excluded from GFED3.1. The model also simulates lower
11 IAV of emissions than GFED3.1, giving a coefficient of variation of 0.05, compared to 0.18 for
12 the GFED3.1 data (0.15 when only natural sources are included in GFED3.1).

13 The interannual variability of fire carbon emissions is known to be partially decoupled from
14 that of burned area (van der Werf et al., 2006), mainly because emission variability is driven by
15 forest fires having higher fuel consumption, whereas burned area variability is driven by savanna
16 fires with relatively large burned fraction but low fuel consumption. At the global scale, the IAV
17 of fire carbon emissions is simulated to be closely related to that of burned area (Fig. S4, giving a
18 correlation coefficient of 0.88 over 1997–2009 – all data detrended). In contrast, the correlation
19 coefficient between GFED3.1 natural source emissions and burned area is 0.52 over the same
20 period (0.04 when emissions from both natural and anthropogenic sources are included), i.e.,
21 smaller than ORCHIDEE-SPITFIRE. Thus the IAV of carbon emissions is more strongly coupled
22 with that of burned area in ORCHIDEE than in GFED3.1, because emissions are dominated by
23 burning of litter (from grassland, savanna and forest) and are less driven by forest fires that
24 involve large amount of live biomass burning.

25 3.2.2 Comparison of simulated carbon emissions with GFED3.1 for different regions

26 Annual fire carbon emissions simulated by ORCHIDEE-SPITFIRE are compared with
27 GFED3.1 data for 1997–2009 for different regions in Fig. 4 (see figure caption for expansion of
28 GFED region abbreviations and Fig. S5 for region distribution). The three regions with the most
29 frequent fires, Northern Hemisphere Africa (NHAF), Southern Hemisphere Africa (SHAF) and
30 Australia (AUST) have total fire emissions of $1.17 \text{ Pg C yr}^{-1}$ and contribute 59% of the global
31 total emissions in GFED3.1. In ORCHIDEE, annual emissions are $1.18 \text{ Pg C yr}^{-1}$ for these three
32 regions; an overestimation in NHAF being partly compensated by underestimation in SHAF.

33 The GFED3.1 data have very low emissions in Temperate North America (TENA), Middle
34 East (MIDE), Central Asia (CEAS) and Europe (EURO) (50 Tg C yr^{-1} in total for the three

1 regions; 2.5% of the global total), whereas ORCHIDEE-SPITFIRE simulates much higher
2 emissions (294 Tg C yr⁻¹; 14% of the global total) possibly because forest fire control measures
3 (Fernandes et al., 2013; Keeley et al., 1999) and forest management in temperate countries (Fang
4 et al., 2001; Luyssaert et al., 2010) are not modelled; this leads to higher burned area and/or higher
5 fuel load in the model. The overestimation of emissions in these three regions is partly driven by
6 the overestimation of burned area (annual burned area of 70.2 Mha yr⁻¹ in the model versus 10.1
7 Mha yr⁻¹ in GFED3.1 in Table 1).

8 The three regions where the model underestimates carbon emissions are Boreal Asia
9 (BOAS), Southeast Asia (SEAS) and Equatorial Asia (EQAS), with simulated emissions of 103
10 Tg C yr⁻¹ (4.9% of the global total), compared with 412 Tg C yr⁻¹ in GFED3.1 (21% of the global
11 total). The low bias of emissions in BOAS and SEAS is explained by the underestimation of
12 burned area (Table 1) whereas for EQAS, underestimates in both burned area and fuel
13 consumption by the model are found (Table 1) (in particular, peat burning that dominates
14 emissions in 1997–98 in SEAS is lacking in the model, see van der Werf et al., 2008). This points
15 to the need to explicitly include deforestation and peat fires, which are associated with a high
16 amount of fuel consumption (van der Werf et al., 2010).

17 3.2.3 Fire fuel consumption and latitudinal pattern of emissions

18 Simulated fuel consumption (g C per m² of area burned) in fire is compared to GFED3.1 data
19 in Fig. 5. Both ORCHIDEE-SPITFIRE and GFED3.1 show a large amount of fuel consumption in
20 boreal regions. But fuel consumption in the Russian boreal forest is smaller in the model than
21 GFED3.1 (simulated 400–2000 g C m⁻² compared to 2000–5000 g C m⁻² in GFED3.1). The model
22 also fails to capture the high fire fuel consumption (5–20 kg C m⁻²) at the southern edge of the
23 Amazonian rainforest and in Southeast Asia, which are associated with deforestation fires or peat
24 fires (see also Fig. 6 and Fig. 13 in van der Werf et al., 2010). The fire fuel consumptions for
25 savannas and woodland savannas in Africa and Australia are higher in the model than GFED3.1,
26 with fuel consumption in northern Africa of 1000–2000 g C m⁻² against 200–1000 g C m⁻² by
27 GFED3.1. In southern Africa, ORCHIDEE produces fuel consumption of 1000–2000 g C m⁻²
28 against only 400–1000 g C m⁻² in GFED3.1. The simulated higher fuel consumption in tropical
29 savannas and woodland savannas might be due to a combination of overestimated fuel load and
30 combustion completeness, which is discussed in more detail in section 3.2.4. Further, we
31 acknowledge the fact that ORCHIDEE can have grass and tree PFTs coexisting on the same grid
32 point, but does not describe woody savannas or miombo forests where grass and trees compete
33 locally for water, light and nutrients and could have lower fuel consumptions due to the presence
34 of fire-resistant tree species (Hoffmann et al., 2012).

35 Figure 6 shows carbon emissions per grid cell area (g C per m² of grid cell) calculated as the
36 product of fire fuel consumption (Fig. 5) and burned fraction (Fig. 2). Because underestimated
37 burned fractions in African and Australian savannas and woodland savannas compensate for

1 overestimated fuel consumption, fire carbon emissions per grid cell for these regions are of similar
2 magnitude to those in GFED3.1. Emissions per grid cell area in southern African woodland
3 savanna are even underestimated by ORCHIDEE ($10\text{--}50\text{ g C m}^{-2}\text{ yr}^{-1}$) compared with GFED3.1
4 ($50\text{--}200\text{ g C m}^{-2}\text{ yr}^{-1}$), due to the great underestimation in burned area.

5 By looking at the latitudinal distribution of burned area and emission, the systematic error in
6 ORCHIDEE's estimated emissions can be clearly related to that in burned area (Fig. 7). The
7 underestimation of burned area in tropical and subtropical regions ($30^{\circ}\text{S}\text{--}15^{\circ}\text{N}$) (Fig. 2) is
8 compensated by the overestimated fire fuel consumption. In southern tropical regions ($30^{\circ}\text{S}\text{--}0^{\circ}$),
9 carbon emissions are still underestimated (by 270 Tg C yr^{-1}) despite this compensation effect,
10 whereas in northern tropical regions ($0^{\circ}\text{--}15^{\circ}\text{N}$), the compensation leads to overestimated
11 emissions (by 190 Tg C yr^{-1}) compared with GFED3.1.

12 3.2.4 Attributing systematic emission errors to burned area and fuel consumption at regional level

13 Table 1 compares mean annual simulated and GFED3.1 emissions for 1997–2009 for
14 different regions. The model bias of emissions is qualitatively attributed to those of burned area
15 and fuel consumption. Table S2 further compares NPP and fire combustion completeness between
16 the model and the GFED3.1 data (where NPP is from the CASA biosphere model, with all
17 GFED3.1 data in Table S2 obtained from Table 4 in van der Werf et al., 2010). For all regions
18 (except NHAF and AUST) where emissions are overestimated by the model (TENA, CEAM,
19 NHSA, SHSA, EURO, MIDE, CEAS), there is a coincident overestimation in burned area, which
20 sometimes overrides the underestimated fuel consumption in regions such as CEAM. Regions
21 where emissions are underestimated also show underestimated burned area (with the exception of
22 BOAS), some of them also having underestimated fuel consumption (EQAS).

23 The simulated NPP regional averages are in general agreement with those from the CASA
24 model reported by van der Werf et al. (2010) (Table S2), indicating that the simulated fuel load
25 might be comparable to GFED3.1 data, and that systematic errors in fuel consumption might be
26 dominated by errors in the combustion completeness of different fuels. On the one hand,
27 simulated combustion completeness for litter agrees well with the values used in GFED3.1; but on
28 the other hand, combustion completeness for the litter and aboveground live biomass combined is
29 much higher in ORCHIDEE than GFED3.1 over BOAS, BONA, MIDE, NHAF, SHAF and
30 AUST, and much lower over EQAS. This might reflect a higher or lower simulated combustion
31 completeness of tree live biomass, which needs further investigation. The higher simulated
32 combustion completeness for litter and live biomass combined in NHAF, SHAF and AUST
33 contributes to the higher fuel consumptions in these regions, given the fact that simulated NPP is
34 rather similar to GFED3.1 over these regions (except for NHAF where the simulated NPP is 40%
35 higher than GFED3.1 and combustion completeness is 2.6 times higher). A recent comparison
36 among different fuel load products by Pettinari et al. (2015, to be submitted) also indicates that
37 our simulated fuel loads in savannas and shrublands are higher than their fuel-model-based data,

1 consistent with the higher NPP in Africa and Australia (Table S2). At the same time, one should
2 also keep in mind that GFED3.1 is not a completely observation dataset, but is another model
3 calculation of fire emissions. Given the availability of the comprehensive fuel combustion field
4 data recently compiled by van Leeuwen et al. (2014), more careful calibration and validation of
5 the simulated combustion completeness for different fuel types could be performed in the future.

6 Finally, the combustion completeness (CC) values used for the 100 and 1000h dead fuel for
7 temperate forests, boreal forests and grasslands are slightly different from those reported by van
8 Leeuwen et al. (2014). The mean CC values for the latter three biomes as updated in van Leeuwen
9 et al. (2014) are 0.69 ± 0.13 , 0.47 ± 0.16 , and 0.81 ± 0.16 respectively. The CC values for boreal
10 forests and grasslands used here are within the uncertainty range by van Leeuwen et al. (2014).
11 The CC value for temperate forests is higher than van Leeuwen et al. (2014). We developed a
12 simple approach to adjust the simulated fire carbon emissions for these three biomes by
13 multiplying the simulated emissions by the ratio of our CC values to those of van Leeuwen et al.
14 (2014), and found that the global total fire carbon emissions remain almost the same (2.1 Pg C yr^{-1}
15 versus $2.08 \text{ Pg C yr}^{-1}$ before and after adjustment for 1997–2009). This is because the smaller CC
16 values used for temperate and boreal forests are compensated for by the larger CC value of
17 grasslands used in the model.

18 3.3 The role of fires in the terrestrial carbon balance

19 3.3.1 The simulated carbon balance for the last decade (1993–2012)

20 Figure 8 shows the percentage of NPP emitted by fire over the last decade (2003–2012).
21 Regions with frequent burning show a higher fraction of NPP being returned to the atmosphere by
22 fire. Yet, heterotrophic respiration remains the dominant pathway for returning NPP to the
23 atmosphere, accounting for 85.7% of the global NPP (91.1% when agricultural harvest is
24 included, the CH term in Eq. 1). Fire carbon emissions account for 3.4% of NPP, with the
25 remaining 5.2% of NPP being accumulated in the biosphere as a carbon sink (NBP) (As
26 mentioned in section 2.3, the remaining positive NBP of $0.19 \text{ Pg C yr}^{-1}$ is subtracted here, taking
27 account for 0.3% of NPP). The simulated global NPP for 2003–2012 is 60 Pg C yr^{-1} in the fireON
28 simulation, with 2.1 Pg C yr^{-1} emitted as fire emissions, and 3.1 Pg C yr^{-1} stored as NBP. The
29 simulated NBP is within the 1-sigma error of the observed residual sink for the same period,
30 which is of $2.8 \pm 0.8 \text{ Pg C yr}^{-1}$ (see Le Quéré et al., 2013 for uncertainty estimation). Fire carbon
31 emissions as a percentage of NPP for 1901–2012 average show little difference with 2003–2012
32 average in terms of spatial distribution, except that the percentages are slightly lower than 2003–
33 2012 average for grassland fires such as in central and eastern Asia (Fig. S6).

1 3.3.2 Fire-induced terrestrial carbon sink reduction for 1901–2012

2 The different components of global carbon fluxes for the fireON and fireOFF simulations are
3 shown in Fig. 9. Net primary production (NPP) for fireON and fireOFF are very similar (NPP is 6
4 Tg C yr^{-1} higher in fireOFF for 1901–2012) (Fig. 9a). This greater NPP in the fireOFF simulation
5 compared with fireON might be underestimated, because land-cover change or vegetation
6 dynamics were ignored in the simulations (For example, bigger forest coverage would have
7 occurred in the fireOFF simulation if vegetation dynamics were modelled).

8 The carbon sink in fireOFF is greater than that in fireON (Fig. 9c). This is because fire
9 emissions ($1.91 \text{ Pg C yr}^{-1}$ for 1901–2012) are greater than the heterotrophic respiration excess in
10 fireOFF (Fig. 9b, by $1.62 \text{ Pg C yr}^{-1}$ averaged over 1901–2012). The fire-induced sink reduction
11 (SR_{fire}) amounts to $0.32 \pm 0.09 \text{ Pg C yr}^{-1}$ over 1901–2012, or 20% of the fireOFF NBP. This sink
12 reduction would have been bigger if deforestation (land-cover change) and peat fires were
13 included in the model because carbon released from these fires is more likely an irreversible net
14 carbon source, i.e., it will not be re-absorbed by post-fire plant recovery on a centennial time
15 scale.

16 The small fire-induced carbon sink reduction obtained in this study, when only natural
17 wildfires are modelled and with static vegetation cover, implies that if carbon stocks in the fuel
18 (dominated by litter or organic soil except in cases of peat and deforestation fires) were not
19 consumed in fires, they would have been decomposed and have contributed to the heterotrophic
20 respiration. This suggests a "fire respiration partial compensation" in the model. I.e., fire carbon
21 emissions are somewhat analogous to heterotrophic respiration, and when fires are extreme their
22 emissions would exceed far their role of respiration compensation, causing a larger net reduction
23 in carbon sink compared to a world without fire. The sink reduction variability is closely
24 correlated with fire emission anomalies during 1901–2012 (with a correlation coefficient of 0.71,
25 Fig. 9d). Fire carbon emissions show an acceleration of 1.8 Tg C yr^{-2} prior to 1970, and a trend of
26 6 Tg C yr^{-2} after 1970, with both trends being significant at the 0.05 level.

27 Our simulated cumulative land carbon sink (NBP) for 1959–2012 is 109.6 Pg C (with 80.8
28 Pg C stored in live biomass and 28.8 Pg C in litter and soil), which is close to the cumulative
29 residual sink of 105.9 Pg C (Le Quéré et al., 2013). The cumulative land sink in fireOFF is 127.2
30 Pg C , suggesting a cumulative sink reduction of 17.6 Pg C by fire since 1959. The correlation
31 coefficient between detrended time series of NBP by the fireON simulation and the residual sink is
32 0.59, indicating that the model is moderately successful at capturing the IAV of the carbon sink by
33 the terrestrial ecosystem.

34 Prentice et al. (2011) pointed out that fire emissions account for one-third and one-fifth of the
35 IAV of the 1997–2005 global carbon balance as indicated by atmospheric inversions, when
36 emissions were from the GFED3.1 data and simulated by the vegetation model LPX, respectively.
37 In our study, fire carbon emissions explained 20% of the IAV of simulated NBP (which is the R^2
38 of the linear regression of detrended annual NBP against simulated carbon emission), congruent

1 with their results.

2 3.3.3 Fire-induced carbon sink reduction for extreme high and low fire years

3 We selected ten “high fire years” years as the ten years with highest global fire-induced sink
4 reduction (SR_{fire}) during 1901–2012 (Fig. 9d), and ten “low fire years” as the years with the ten
5 lowest global SR_{fire} during the same period. The average SR_{fire} for the high fire years is 0.49 Pg C
6 yr^{-1} (23% of the fireOFF NBP), compared with an average SR_{fire} of $0.17 \text{ Pg C yr}^{-1}$ (7% of the
7 fireOFF NBP) for the ten low fire years.

8 The Pearson correlation coefficient (r) between the SR_{fire} time series and other model
9 variable or climatic drivers (temperature, precipitation) was used to investigate the driving factors
10 for fire-induced sink reduction. The SR_{fire} variation was found to be best explained by fire
11 numbers ($r = 0.65$, $p < 0.05$) within the model, since fire numbers are also driving the variation of
12 burned area ($r = 0.81$, $p < 0.05$). SR_{fire} is also positively correlated with land surface temperature
13 ($r = 0.16$, $p = 0.08$), and negatively correlated with precipitation ($r = -0.23$, $p < 0.05$), although the
14 correlation is fairly weak.

15 The opposite of SR_{fire} is positively correlated with the Southern Oscillation Index (SOI) ($r =$
16 0.29 , $p < 0.05$, Fig. 10), suggesting that global fire-induced sink reduction is significantly related
17 to the change in the tropical Pacific sea-surface temperature gradient, because of its strong
18 influence over global rainfall (Ropelewski and Halpert, 1987, 1996). The El Niño state (i.e., low
19 SOI value) of climate oscillation generally coincides with larger sink reduction by fires (i.e., larger
20 SR_{fire}), and La Niña with smaller reduction. Indeed, seven out of the ten high fire years occur
21 during El Niño episodes, and six out of the ten low fire years occur during La Niña episodes (The
22 diagnosis of El Niño and La Niña episodes is given by the Bureau of Meteorology of Australian
23 government, <http://www.bom.gov.au/climate/enso/Inlist/>). SR_{fire} is more strongly related with SOI
24 in tropical regions than at the global scale thanks to the more direct impacts of ENSO events (for
25 30°S – 30°N , the relationship between $-SR_{\text{fire}}$ and SOI yields $r = 0.33$ with $p < 0.05$). This region
26 contributes 82 and 72% of global total emissions and carbon sink, respectively.

27 As we did not include agricultural fires, deforestation fires and peat fires in our simulation,
28 the analysis of fire-induced sink reduction related to climate variations presented here mainly
29 represents a scenario of naturally occurring fires. Globally, the 1997-1998 fire emissions anomaly
30 is underestimated in the model, principally related to the fact that the anthropogenic peatland and
31 deforestation burning in tropical Asia and America (Field et al., 2009; Page et al., 2002; van der
32 Werf et al., 2004, 2010) are not included. The underestimated IAV in fire carbon emissions by the
33 model might lead to underestimated temporal variability in SR_{fire} , thus the actual correlation
34 between fire-induced sink reduction and SOI over the historical period might be underestimated.

35 Despite the fact that systematic bias exists for simulated burned area, as global total fire
36 carbon emissions are constrained with GFED3.1 estimate, the estimated long-term average SR_{fire}
37 remains reliable. To verify this, we forced the model with observed GFED3.1 burned area data for

1 1997-2009 on a monthly time step and used the regional specific combustion completeness values
2 as reported in van der Werf et al., 2010 (Table 4 in van der Werf et al., 2010 for the 14 regions).
3 The forced simulation yields annual global fire carbon emissions of 1.8 Pg C yr⁻¹ for 1997-2009
4 and an SR_{fire} of 0.39 Pg C yr⁻¹, close to the fire emissions of 2.1 Pg C yr⁻¹ and SR_{fire} of 0.36 Pg C
5 yr⁻¹ as given by the prognostic simulation.

6 The suggested "respiration partial compensation" by fires (i.e., larger sink reduction with
7 more extreme fires), and the strong relevance of SR_{fire} to climatic variations (i.e., larger sink
8 reduction during warm and dry El Niño years) have implications for the future role of fires in the
9 terrestrial carbon balance. Studies show that climate warming in recent decades has already driven
10 boreal fire frequency to exceed its historical limit (Kelly et al., 2013) and resulted in increased
11 carbon loss (Hayes et al., 2011; Mack et al., 2011; Turetsky et al., 2011). The ENSO-driven
12 climate variability, with its strong influence on global precipitation, has widespread impact on fire
13 activity across the globe (Carmona-Moreno et al., 2005; Kitzberger et al., 2001; Chen et al., 2011;
14 Prentice et al., 2011). With continuing anthropogenic disturbances on the climate system by
15 greenhouse gas emissions, the evidence from multiple-modelling exercises indicates a likely
16 increase in the frequency of extreme El Niño events and droughts in the 21st century (Cai et al.,
17 2014; Meehl and Washington, 1996; Prudhomme et al., 2013; Timmermann et al., 1999). These
18 projections in turn lead to projected increases in fire activities and emissions (Flannigan et al.,
19 2009; Kloster et al., 2012). As a further consequence, the capacity for land ecosystems to
20 sequester carbon is likely to be further diminished in the future.

21 3.3.4 Simulated fire-induced sink reduction and comparison with Li et al.

22 Li et al. (2014) investigated the role of fires in the terrestrial carbon cycle using the CLM4.5
23 model and a similar modelling approach (fire-on versus fire-off simulations, with prescribed
24 historical land cover and a de-activated dynamic vegetation module). They found that fires
25 reduced the terrestrial carbon sink by on average 1.0 Pg C yr⁻¹ during the 20th century. Our
26 simulated sink reduction (0.32 Pg C yr⁻¹ for 1901–2012) is smaller than theirs. However, fire
27 carbon emissions (called the *fire direct effect* by Li et al., 2014) from the two studies are similar
28 (1.9 Pg C yr⁻¹ by both studies for the 20th century). Therefore, the difference in fire sink reduction
29 between the two studies must be due to differences in other flux estimates (NPP and heterotrophic
30 respiration).

31 Li et al. (2014) estimated that fire reduced global NPP by 1.9 Pg C yr⁻¹, but the heterotrophic
32 respiration was reduced by an even larger amount (2.7 Pg C yr⁻¹), resulting in a higher NEP of 0.9
33 Pg C yr⁻¹ in their fire-off simulation (called *fire indirect effect*). We also find a higher heterotrophic
34 respiration in our fireOFF simulation (by on average 1.62 Pg C yr⁻¹ over 1901–2012) but the
35 simulated NPP difference is negligible (6 Tg C yr⁻¹ higher in fireOFF than fireON). The NPP
36 reduction by fire is probably underestimated in our study, because land-cover change fires are not
37 accounted for, and grassland or agricultural land converted from forest has much lower NPP than

1 it had prior to conversion (Houghton et al., 1999). Thus the NEP increase by switching fire off
2 might also be underestimated, which leads to underestimated sink reduction by fire.

3 Lastly, our study shares two prominent uncertainties in quantifying the role of fires in the
4 terrestrial carbon cycle with those discussed by Li et al. (2014). Firstly, the vegetation dynamics
5 module was switched off in our simulation, and this might limit the terrestrial carbon sink by land
6 ecosystems in a world without fire. Previous studies have pointed out that if all fires were
7 suppressed tree cover would expand in regions where current grassland or woodland ecosystems
8 are maintained by fires (Bond et al., 2005; Staver et al., 2011); and that the expanded forest
9 coverage would increase land carbon stock (Bond et al., 2005). Secondly, because ORCHIDEE
10 was not coupled to an atmosphere model, the atmospheric concentration changes for various gases
11 released by fire, or a complete fire-vegetation-climate feedback, as discussed in the Introduction,
12 were not included.

13 3.3.5 The role of fires in the terrestrial carbon balance in relation to fire pyromes

14 We compared fire fuel consumption, the fraction of NPP returned via fire emissions and its
15 temporal variation, and carbon sink efficiencies (SE) for fireOFF and fireON simulations for the
16 five pyromes defined by Archibald et al. (2013) (see Sect. 2.5). The temporal variation for the
17 fraction of NPP lost to fire emissions is examined as the coefficient of variation during 1901–
18 2012, which is the standard deviation divided by the mean.

19 According to model simulation, Frequent–Intense–Large (FIL) and Frequent–Cool–Small
20 (FCS) fires have higher fuel consumption than infrequent Rare–Intense–Large (RIL) and Rare–
21 Cool–Small (RCS) fires (Fig. 11), fuel consumption being the highest in the FCS pyrome (1.2 kg
22 C m⁻²) and the lowest in the RCS pyrome (0.6 kg C m⁻²). Correspondingly, the ratio of fire
23 emissions to NPP is also higher in frequent-fire pyromes than in infrequent ones, but the temporal
24 variation of this fraction is higher for RCS and RIL pyromes. Regions with infrequent fires (RCS,
25 RIL and ICS) have greater sink efficiency than those with frequent ones (FIL, FCS) for the
26 fireOFF simulation. This pattern remains for the fireON simulation, which gives smaller sink
27 efficiency than fireOFF for all the pyromes, due to the adverse effects of fires on the land carbon
28 sink. Consequently, the sink efficiency as reduced by fires remains higher in infrequent-fire
29 pyromes (being the highest in the RIL pyrome) than frequent ones (being the lowest in the FIL
30 pyrome).

31 It is reasonable to find that frequent fires have higher fuel consumption than small cool ICS
32 and RCS fires, because the latter are generally human-controlled burning with limited fuel load
33 (Archibald et al., 2013). However, intuitively, the Rare–Intense–Large (RIL) fires are expected to
34 have at least comparable, if not larger, fuel consumption than the FIL and FCS pyromes, since
35 their spatial extent covers the North American boreal forest biome where large amounts of soil
36 (and biomass) carbon stocks are exposed to burning. Our model simulation does show a high
37 amount of fire fuel consumption in North American boreal forests: 1–5 kg C m⁻² (Fig. 5),

1 comparable to that reported in regional studies (French et al., 2011; Kasischke and Hoy, 2012). A
2 closer examination of the fire pyrome distribution map (Fig. S2) reveals that some of the grassland
3 fires in central and eastern Asia and inland Australia are also classified as RIL fires, which have a
4 rather low simulated fuel consumption rate (1–200 g C m⁻², Fig. 5). Thus the simulated fuel
5 consumption for RIL fires is a mean value for all above regions (including boreal forests in
6 Eurasia as well), which is lower than frequent fires.

7 We also find the carbon sink efficiencies for infrequent-fire pyromes are higher than frequent
8 ones for both fireON and fireOFF simulations, probably because more forests are located in
9 infrequent-fire pyromes (Table 1 in Archibald et al., 2013). The sink efficiency reduction (SE_{OFF}-
10 SE_{ON}) by fires is the highest in the RIL pyrome, congruent with a higher Emission-to-NPP
11 fraction. If we examine the percentage of fire-induced sink efficiency reduction to SE_{OFF}, the FIL,
12 FCS and RIL pyromes emerge again to have higher percentage than RCS and ICS pyromes (data
13 not shown). This indicates that frequent fires and infrequent-large fires reduce the carbon
14 sequestration capacity of land ecosystems to a higher extent. Note that as an initial attempt to
15 understand the role of fires in carbon cycling for different pyromes (such as that for different
16 biomes), great uncertainties exist in the modelling results presented here. Sources of uncertainties
17 include that agricultural and deforestation fires were included in Archibald et al. (2013) but not in
18 our model; errors and uncertainties exist in simulated fire fuel consumption and fire emissions; the
19 combustion difference between surface fires in boreal Eurasian forests and crown fires in North
20 American boreal forests (de Groot et al., 2013; Wirth, 2005) is lacking in the model; uncertainties
21 exist in the classification of fire pyromes.

22 **4 Summary and conclusions**

23 In this study, we used the ORCHIDEE land surface model with recently integrated SPITFIRE
24 model to estimate the role of fires in the terrestrial carbon balance for the 20th century. The
25 simulated global fire carbon emissions for 1997–2009 are 2.1 Pg C yr⁻¹, close to the 2.0 Pg C yr⁻¹
26 as estimated by the GFED3.1 data (when all types of fires are included), owing to error
27 compensation among different regions in the model. Fire carbon emissions are mainly
28 underestimated in southern hemisphere tropical regions and this error is compensated by an
29 overestimation in temperate ecosystems. The regional emission errors are found to be coincident
30 with the errors in simulated burned area, with the exception that fire fuel consumption is
31 underestimated in regions featuring peatland or deforestation fires such as equatorial Asia, because
32 these fires are not explicitly included in the model.

33 Fires reduced the terrestrial carbon uptake by an average of 0.32 Pg C yr⁻¹ over the period
34 1901–2012, equivalent to 20% of the carbon sink in a world without fire. Our simulations suggest
35 that fires have a "respiration partial compensation" (although the inclusion of dynamic vegetation
36 in the model might change this). Fire emissions in low fire years mainly compensate for
37 heterotrophic respiration that would occur without fire combustion, but emissions in extreme high

1 fire years exceed far their "respiration partial compensation" and create larger reduction in the
2 terrestrial carbon sink. This fire-induced sink reduction has been found to be significantly
3 correlated with climatic variations including El Niño Southern Oscillation (ENSO), with larger
4 sink reductions occurring in warm, dry conditions. This finding has an important implication for
5 the future role of fires in the terrestrial carbon balance, because the capacity of terrestrial
6 ecosystems to sequester carbon will be more likely diminished in a future climate with more
7 frequent and intense droughts and more extreme El Niño events. This also implies that fires might
8 significantly impact the climate-carbon response (known as the γ factor) as simulated by coupled
9 climate-carbon models.

10
11 *Acknowledgements* We thank S. Archibald for providing the fire pyrome distribution map.
12 Moreover, we thank the two anonymous reviewers for providing valuable comments which
13 improved the quality of the manuscript. Funding for this work was provided by the ESA firecci
14 project (<http://www.esa-fire-cci.org/>) and EU FP7 project PAGE21.

15 **References**

16 Archibald, S., Lehmann, C. E. R., Gómez-Dans, J. L. and Bradstock, R. A.: Defining pyromes and
17 global syndromes of fire regimes, *Proc. Natl. Acad. Sci. U.S.A.*, 110(16), 6442–6447,
18 doi:10.1073/pnas.1211466110, 2013.

19 Balshi, M. S., McGuire, A. D., Duffy, P., Flannigan, M., Kicklighter, D. W. and Melillo, J.:
20 Vulnerability of carbon storage in North American boreal forests to wildfires during the 21st
21 century, *Global Change Biol.*, 15, 1491–1510, 2009.

22 Beck, P. S. A., Goetz, S. J., Mack, M. C., Alexander, H. D., Jin, Y., Randerson, J. T. and Lorant,
23 M. M.: The impacts and implications of an intensifying fire regime on Alaskan boreal forest
24 composition and albedo, *Global Change Biol.*, 17(9), 2853–2866, doi:10.1111/j.1365-
25 2486.2011.02412.x, 2011.

26 Bond, W. J., Woodward, F. I. and Midgley, G. F.: The global distribution of ecosystems in a
27 world without fire, *New Phytol.*, 165(2), 525–537, doi:10.1111/j.1469-8137.2004.01252.x, 2005.

28 Bowman, D. M. J. S., Balch, J. K., Artaxo, P., Bond, W. J., Carlson, J. M., Cochrane, M. A.,
29 D'Antonio, C. M., DeFries, R. S., Doyle, J. C., Harrison, S. P., Johnston, F. H., Keeley, J. E.,
30 Krawchuk, M. A., Kull, C. A., Marston, J. B., Moritz, M. A., Prentice, I. C., Roos, C. I., Scott, A.
31 C., Swetnam, T. W., van der Werf, G. R. and Pyne, S. J.: Fire in the Earth System, *Science*,
32 324(5926), 481–484, doi:10.1126/science.1163886, 2009.

33 Cai, W., Borlace, S., Lengaigne, M., van Rensch, P., Collins, M., Vecchi, G., Timmermann, A.,
34 Santoso, A., McPhaden, M. J., Wu, L., England, M. H., Wang, G., Guilyardi, E. and Jin, F.-F.:
35 Increasing frequency of extreme El Niño events due to greenhouse warming, *Nature Clim.*
36 *Change*, 4(2), 111–116, doi:10.1038/nclimate2100, 2014.

37 Carmona-Moreno, C., Belward, A., Malingreau, J.-P., Hartley, A., Garcia-Alegre, M.,
38 Antonovskiy, M., Buchshtaber, V. and Pivovarov, V.: Characterizing interannual variations in
39 global fire calendar using data from Earth observing satellites, *Global Change Biol.*, 11(9), 1537–
40 1555, doi:10.1111/j.1365-2486.2005.01003.x, 2005.

41 Chen, Y., Randerson, J. T., Morton, D. C., DeFries, R. S., Collatz, G. J., Kasibhatla, P. S., Giglio,
42 L., Jin, Y. and Marlier, M. E.: Forecasting Fire Season Severity in South America Using Sea
43 Surface Temperature Anomalies, *Science*, 334(6057), 787–791, doi:10.1126/science.1209472,

- 1 2011.
- 2 Chuvieco, E., Giglio, L. and Justice, C.: Global characterization of fire activity: toward defining
3 fire regimes from Earth observation data, *Global Change Biol.*, 14, 1488–1502, 2008.
- 4 Dufresne, J.-L., Foujols, M.-A., Denvil, S., Caubel, A., Marti, O., Aumont, O., Balkanski, Y.,
5 Bekki, S., Bellenger, H., Benshila, R., Bony, S., Bopp, L., Braconnot, P., Brockmann, P., Cadule,
6 P., Cheruy, F., Codron, F., Cozic, A., Cugnet, D., Noblet, N. de, Duvel, J.-P., Ethé, C., Fairhead,
7 L., Fichet, T., Flavoni, S., Friedlingstein, P., Grandpeix, J.-Y., Guez, L., Guilyardi, E.,
8 Hauglustaine, D., Hourdin, F., Idelkadi, A., Ghattas, J., Joussaume, S., Kageyama, M., Krinner,
9 G., Labetoulle, S., Lahellec, A., Lefebvre, M.-P., Lefevre, F., Levy, C., Li, Z. X., Lloyd, J., Lott,
10 F., Madec, G., Mancip, M., Marchand, M., Masson, S., Meurdesoif, Y., Mignot, J., Musat, I.,
11 Parouty, S., Polcher, J., Rio, C., Schulz, M., Swingedouw, D., Szopa, S., Talandier, C., Terray, P.,
12 Viovy, N. and Vuichard, N.: Climate change projections using the IPSL-CM5 Earth System
13 Model: from CMIP3 to CMIP5, *Clim.Dyn.*, 40(9-10), 2123–2165, doi:10.1007/s00382-012-1636-
14 1, 2013.
- 15 Fang, J., Chen, A., Peng, C., Zhao, S. and Ci, L.: Changes in Forest Biomass Carbon Storage in
16 China Between 1949 and 1998, *Science*, 292(5525), 2320–2322, doi:10.1126/science.1058629,
17 2001.
- 18 Fernandes, P. M., Davies, G. M., Ascoli, D., Fernández, C., Moreira, F., Rigolot, E., Stoof, C. R.,
19 Vega, J. A. and Molina, D.: Prescribed burning in southern Europe: developing fire management
20 in a dynamic landscape, *Frontiers in Ecology and the Environment*, 11(s1), e4–e14,
21 doi:10.1890/120298, 2013.
- 22 Flannigan, M. D., Krawchuk, M. A., de Groot, W. J., Wotton, B. M. and Gowman, L. M.:
23 Implications of changing climate for global wildland fire, *Int. J. Wildland Fire*, 18(5), 483–507,
24 2009.
- 25 French, N. H. F., de Groot, W. J., Jenkins, L. K., Rogers, B. M., Alvarado, E., Amiro, B., de Jong,
26 B., Goetz, S., Hoy, E., Hyer, E., Keane, R., Law, B. E., McKenzie, D., McNulty, S. G., Ottmar,
27 R., Pérez-Salicrup, D. R., Randerson, J., Robertson, K. M. and Turetsky, M.: Model comparisons
28 for estimating carbon emissions from North American wildland fire, *J. Geophys. Res.*, B, 116(G4),
29 G00K05, doi:10.1029/2010JG001469, 2011.
- 30 Giglio, L., Randerson, J. T., van der Werf, G. R., Kasibhatla, P. S., Collatz, G. J., Morton, D. C.
31 and DeFries, R. S.: Assessing variability and long-term trends in burned area by merging multiple
32 satellite fire products, *Biogeosciences*, 7(3), 1171–1186, doi:10.5194/bg-7-1171-2010, 2010.
- 33 Gill, A. M. and Allan, G.: Large fires, fire effects and the fire-regime concept, *Int. J. Wildland
34 Fire*, 17(6), 688–695, 2008.
- 35 De Groot, W. J., Cantin, A. S., Flannigan, M. D., Soja, A. J., Gowman, L. M. and Newbery, A.: A
36 comparison of Canadian and Russian boreal forest fire regimes, *Forest Ecology and Management*,
37 294, 23–34, doi:10.1016/j.foreco.2012.07.033, 2013.
- 38 Field, R. D., Werf, G. R. van der and Shen, S. S. P.: Human amplification of drought-induced
39 biomass burning in Indonesia since 1960, *Nat. Geosci.*, 2(3), 185–188, doi:10.1038/ngeo443,
40 2009.
- 41 Hayes, D. J., McGuire, A. D., Kicklighter, D. W., Gurney, K. R., Burnside, T. J. and Melillo, J.
42 M.: Is the northern high-latitude land-based CO₂ sink weakening?, *Global Biogeochem. Cycles*,
43 25(3), GB3018, doi:10.1029/2010GB003813, 2011.
- 44 Hoffmann, W. A., Geiger, E. L., Gotsch, S. G., Rossatto, D. R., Silva, L. C., Lau, O. L.,
45 Haridasan, M. and Franco, A. C.: Ecological thresholds at the savanna-forest boundary: how plant

- 1 traits, resources and fire govern the distribution of tropical biomes, *Ecol. Lett.*, 15(7), 759–768,
2 2012.
- 3 Houghton, R. A., Hackler, J. L. and Lawrence, K. T.: The U.S. Carbon Budget: Contributions
4 from Land-Use Change, *Science*, 285(5427), 574–578, doi:10.1126/science.285.5427.574, 1999.
- 5 Jin, Y., Randerson, J. T., Goetz, S. J., Beck, P. S. A., Loranty, M. M. and Goulden, M. L.: The
6 influence of burn severity on postfire vegetation recovery and albedo change during early
7 succession in North American boreal forests, *J. Geophys. Res.*, B, 117(G1), G01036,
8 doi:10.1029/2011JG001886, 2012.
- 9 Jung, M., Reichstein, M., Margolis, H. A., Cescatti, A., Richardson, A. D., Arain, M. A., Arneth,
10 A., Bernhofer, C., Bonal, D., Chen, J., Gianelle, D., Gobron, N., Kiely, G., Kutsch, W., Lasslop,
11 G., Law, B. E., Lindroth, A., Merbold, L., Montagnani, L., Moors, E. J., Papale, D., Sottocornola,
12 M., Vaccari, F. and Williams, C.: Global patterns of land-atmosphere fluxes of carbon dioxide,
13 latent heat, and sensible heat derived from eddy covariance, satellite, and meteorological
14 observations, *J. Geophys. Res.*, B, 116(G3), G00J07, doi:10.1029/2010JG001566, 2011.
- 15 Kasischke, E. S. and Hoy, E. E.: Controls on carbon consumption during Alaskan wildland fires,
16 *Global Change Biol.*, 18(2), 685–699, doi:10.1111/j.1365-2486.2011.02573.x, 2012.
- 17 Keeley, J. E., Fotheringham, C. J. and Morais, M.: Reexamining Fire Suppression Impacts on
18 Brushland Fire Regimes, *Science*, 284(5421), 1829–1832, doi:10.1126/science.284.5421.1829,
19 1999.
- 20 Kelly, R., Chipman, M. L., Higuera, P. E., Stefanova, I., Brubaker, L. B. and Hu, F. S.: Recent
21 burning of boreal forests exceeds fire regime limits of the past 10,000 years, *Proc. Natl. Acad. Sci.*
22 U.S.A., 110(32), 13055–13060, doi:10.1073/pnas.1305069110, 2013.
- 23 Kiladis, G. N. and Diaz, H. F.: Global Climatic Anomalies Associated with Extremes in the
24 Southern Oscillation, *Journal of Climate*, 2(9), 1069–1090, doi:10.1175/1520-
25 0442(1989)002<1069:GCAAWE>2.0.CO;2, 1989.
- 26 Kitzberger, T., Swetnam, T. W. and Veblen, T. T.: Inter-hemispheric synchrony of forest fires and
27 the El Niño-Southern Oscillation, *Global Ecology and Biogeography*, 10(3), 315–326,
28 doi:10.1046/j.1466-822X.2001.00234.x, 2001.
- 29 Kloster, S., Mahowald, N. M., Randerson, J. T. and Lawrence, P. J.: The impacts of climate, land
30 use, and demography on fires during the 21st century simulated by CLM-CN, *Biogeosciences*, 9,
31 509–525, doi:10.5194/bg-9-509-2012, 2012.
- 32 Kloster, S., Mahowald, N. M., Randerson, J. T., Thornton, P. E., Hoffman, F. M., Levis, S.,
33 Lawrence, P. J., Feddema, J. J., Oleson, K. W. and Lawrence, D. M.: Fire dynamics during the
34 20th century simulated by the Community Land Model, *Biogeosciences*, 7(6), 1877–1902, 2010.
- 35 Krinner, G., Viovy, N., de Noblet-Ducoudré, N., Ogée, J., Polcher, J., Friedlingstein, P., Ciais, P.,
36 Sitch, S. and Prentice, I. C.: A dynamic global vegetation model for studies of the coupled
37 atmosphere-biosphere system, *Global Biogeochem. Cycles*, 19(1), GB1015,
38 doi:10.1029/2003GB002199, 2005.
- 39 Langenfelds, R. L., Francey, R. J., Pak, B. C., Steele, L. P., Lloyd, J., Trudinger, C. M. and
40 Allison, C. E.: Interannual growth rate variations of atmospheric CO₂ and its $\delta^{13}\text{C}$, H₂, CH₄, and
41 CO between 1992 and 1999 linked to biomass burning, *Global Biogeochem. Cycles*, 16(3), 21–1–
42 21–22, doi:10.1029/2001GB001466, 2002.
- 43 Van Leeuwen, T. T., van der Werf, G. R., Hoffmann, A. A., Detmers, R. G., Rucker, G., French,
44 N. H. F., Archibald, S., Carvalho Jr., J. A., Cook, G. D., de Groot, W. J., Hély, C., Kasischke, E.

- 1 S., Kloster, S., McCarty, J. L., Pettinari, M. L., Savadogo, P., Alvarado, E. C., Boschetti, L.,
2 Manuri, S., Meyer, C. P., Siegert, F., Trollope, L. A. and Trollope, W. S. W.: Biomass burning
3 fuel consumption rates: a field measurement database, *Biogeosciences*, 11(24), 7305–7329,
4 doi:10.5194/bg-11-7305-2014, 2014.
- 5 Li, F., Bond-Lamberty, B. and Levis, S.: Quantifying the role of fire in the Earth system – Part 2:
6 Impact on the net carbon balance of global terrestrial ecosystems for the 20th century,
7 *Biogeosciences*, 11(5), 1345–1360, doi:10.5194/bg-11-1345-2014, 2014.
- 8 Li, F., Levis, S. and Ward, D. S.: Quantifying the role of fire in the Earth system – Part 1:
9 Improved global fire modeling in the Community Earth System Model (CESM1), *Biogeosciences*,
10 10(4), 2293–2314, doi:10.5194/bg-10-2293-2013, 2013.
- 11 Liu, H. and Randerson, J. T.: Interannual variability of surface energy exchange depends on stand
12 age in a boreal forest fire chronosequence, *J. Geophys. Res.*, 113(G1), G01006,
13 doi:10.1029/2007JG000483, 2008.
- 14 Liu, J., Wang, B., Cane, M. A., Yim, S.-Y. and Lee, J.-Y.: Divergent global precipitation changes
15 induced by natural versus anthropogenic forcing, *Nature*, 493(7434), 656–659,
16 doi:10.1038/nature11784, 2013.
- 17 Luysaert, S., Ciais, P., Piao, S. L., Schulze, E.-D., Jung, M., Zaehle, S., Schelhaas, M. J.,
18 Reichstein, M., Churkina, G., Papale, D., Abril, G., Beer, C., Grace, J., Loustau, D., Matteucci, G.,
19 Magnani, F., Nabuurs, G. J., Verbeeck, H., Sulkava, M., Van Der WERF, G. R., Janssens, I. A.
20 and Team, members of the C.-I. S.: The European carbon balance. Part 3: forests, *Global Change*
21 *Biol.*, 16(5), 1429–1450, doi:10.1111/j.1365-2486.2009.02056.x, 2010.
- 22 Mack, M. C., Bret-Harte, M. S., Hollingsworth, T. N., Jandt, R. R., Schuur, E. A. G., Shaver, G.
23 R. and Verbyla, D. L.: Carbon loss from an unprecedented Arctic tundra wildfire, *Nature*,
24 475(7357), 489–492, doi:10.1038/nature10283, 2011.
- 25 Magi, B. I., Rabin, S., Shevliakova, E. and Pacala, S.: Separating agricultural and non-agricultural
26 fire seasonality at regional scales, *Biogeosciences*, 9(8), 3003–3012, doi:10.5194/bg-9-3003-2012,
27 2012.
- 28 Marlier, M. E., DeFries, R., Pennington, D., Nelson, E., Ordway, E. M., Lewis, J., Koplitz, S. N.
29 and Mickley, L. J.: Future fire emissions associated with projected land use change in Sumatra,
30 *Glob. Change Biol.*, 21(1), 345–362, doi:10.1111/gcb.12691, 2015.
- 31 Meehl, G. A. and Washington, W. M.: El Niño-like climate change in a model with increased
32 atmospheric CO₂ concentrations, *Nature*, 382(6586), 56–60, doi:10.1038/382056a0, 1996.
- 33 Mouillot, F. and Field, C. B.: Fire history and the global carbon budget: a 1 degrees x 1 degrees
34 fire history reconstruction for the 20th century, *Global Change Biol.*, 11, 398–420,
35 doi:10.1111/j.1365-2486.2005.00920.x, 2005.
- 36 Page, S. E., Siegert, F., Rieley, J. O., Boehm, H.-D. V., Jaya, A. and Limin, S.: The amount of
37 carbon released from peat and forest fires in Indonesia during 1997, *Nature*, 420(6911), 61–65,
38 doi:10.1038/nature01131, 2002.
- 39 Peterson, D. L. and Ryan, K. C.: Modeling postfire conifer mortality for long-range planning,
40 *Environ. Manage.*, 10, 797–808, doi:10.1007/BF01867732, 1986.
- 41 Pettinari M. L. and Chuvieco E.: Development of a global fuel map using the Fuel Characteristic
42 Classification System. To be submitted to *Glob. Ecol. Biogeogr.*.
- 43 Piao, S., Sitch, S., Ciais, P., Friedlingstein, P., Peylin, P., Wang, X., Ahlström, A., Anav, A.,

- 1 Canadell, J. G., Cong, N., Huntingford, C., Jung, M., Levis, S., Levy, P. E., Li, J., Lin, X., Lomas,
2 M. R., Lu, M., Luo, Y., Ma, Y., Myneni, R. B., Poulter, B., Sun, Z., Wang, T., Viovy, N., Zaehle,
3 S. and Zeng, N.: Evaluation of terrestrial carbon cycle models for their response to climate
4 variability and to CO₂ trends, *Global Change Biol.*, 19(7), 2117–2132, doi:10.1111/gcb.12187,
5 2013.
- 6 Podgorny, I. A., Li, F. and Ramanathan, V.: Large Aerosol Radiative Forcing due to the 1997
7 Indonesian Forest Fire, *Geophys. Res. Lett.*, 30(1), 1028, doi:10.1029/2002GL015979, 2003.
- 8 Prentice, I. C., Kelley, D. I., Foster, P. N., Friedlingstein, P., Harrison, S. P. and Bartlein, P. J.:
9 Modeling fire and the terrestrial carbon balance, *Global Biogeochem. Cycles*, 25, GB3005,
10 doi:10.1029/2010GB003906, 2011.
- 11 Prudhomme, C., Giuntoli, I., Robinson, E. L., Clark, D. B., Arnell, N. W., Dankers, R., Fekete, B.
12 M., Franssen, W., Gerten, D., Gosling, S. N., Hagemann, S., Hannah, D. M., Kim, H., Masaki, Y.,
13 Satoh, Y., Stacke, T., Wada, Y. and Wisser, D.: Hydrological droughts in the 21st century,
14 hotspots and uncertainties from a global multimodel ensemble experiment, *Proc. Natl. Acad. Sci.*
15 U.S.A., 201222473, doi:10.1073/pnas.1222473110, 2013.
- 16 Pyne, S. J., Andrews, P. L., and Laven, R. D.: *Introduction to wildland fire*, 2 edition, Wiley, New
17 York, 769 pp., 1996.
- 18 Le Quéré, C., Andres, R. J., Boden, T., Conway, T., Houghton, R. A., House, J. I., Marland, G.,
19 Peters, G. P., van der Werf, G. R., Ahlström, A., Andrew, R. M., Bopp, L., Canadell, J. G., Ciais,
20 P., Doney, S. C., Enright, C., Friedlingstein, P., Huntingford, C., Jain, A. K., Jourdain, C., Kato,
21 E., Keeling, R. F., Klein Goldewijk, K., Levis, S., Levy, P., Lomas, M., Poulter, B., Raupach, M.
22 R., Schwinger, J., Sitch, S., Stocker, B. D., Viovy, N., Zaehle, S. and Zeng, N.: The global carbon
23 budget 1959–2011, *Earth Syst. Sci. Data*, 5(1), 165–185, 2013.
- 24 Randerson, J. T., Chen, Y., van der Werf, G. R., Rogers, B. M. and Morton, D. C.: Global burned
25 area and biomass burning emissions from small fires, *J. Geophys. Res.*, B, 117(G4), G04012,
26 doi:10.1029/2012JG002128, 2012.
- 27 Rocha, A. V. and Shaver, G. R.: Postfire energy exchange in arctic tundra: the importance and
28 climatic implications of burn severity, *Global Change Biol.*, 17(9), 2831–2841,
29 doi:10.1111/j.1365-2486.2011.02441.x, 2011.
- 30 Rogers, A.: The use and misuse of $V_{c,max}$ in Earth System Models, *Photosynth Res*, 119(1-2),
31 15–29, doi:10.1007/s11120-013-9818-1, 2014.
- 32 Ropelewski, C. F. and Halpert, M. S.: Global and Regional Scale Precipitation Patterns Associated
33 with the El Niño/Southern Oscillation, *Mon. Wea. Rev.*, 115(8), 1606–1626, doi:10.1175/1520-
34 0493(1987)115<1606:GARSPP>2.0.CO;2, 1987.
- 35 Ropelewski, C. F. and Halpert, M. S.: Quantifying Southern Oscillation-Precipitation
36 Relationships, *J. Climate*, 9(5), 1043–1059, doi:10.1175/1520-
37 0442(1996)009<1043:QSOPR>2.0.CO;2, 1996.
- 38 Rothermel, R. C.: A mathematical model for predicting fire spread in wildland fuels, *Res. Pap.*
39 INT-115, Ogden, UT: U.S. Department of Agriculture, Intermountain Forest and Range
40 Experiment Station, 40 pp., available at: http://www.fs.fed.us/rm/pubs_int/int_rp115.pdf (last
41 access: 30 September 2014), 1972.
- 42 Roy, D. P., Boschetti, L., Justice, C. O. and Ju, J.: The collection 5 MODIS burned area product --
43 Global evaluation by comparison with the MODIS active fire product, *Remote Sensing of*
44 *Environment*, 112(9), 3690–3707, doi:10.1016/j.rse.2008.05.013, 2008.

- 1 Schimel, D. and Baker, D.: Carbon cycle: The wildfire factor, *Nature*, 420(6911), 29–30,
2 doi:10.1038/420029a, 2002.
- 3 Seiler, W. and Crutzen, P. J.: Estimates of gross and net fluxes of carbon between the biosphere
4 and the atmosphere from biomass burning, *Clim. Change*, 2(3), 207–247,
5 doi:10.1007/BF00137988, 1980.
- 6 Staver, A. C., Archibald, S. and Levin, S. A.: The Global Extent and Determinants of Savanna and
7 Forest as Alternative Biome States, *Science*, 334(6053), 230–232, doi:10.1126/science.1210465,
8 2011.
- 9 Tansey, K., Grégoire, J.-M., Defourny, P., Leigh, R., Pekel, J.-F., van Bogaert, E. and
10 Bartholomé, E.: A new, global, multi-annual (2000–2007) burnt area product at 1 km resolution,
11 *Geophys. Res. Lett.*, 35(1), doi:10.1029/2007GL031567, 2008.
- 12 Thonicke, K., Spessa, A., Prentice, I. C., Harrison, S. P., Dong, L. and Carmona-Moreno, C.: The
13 influence of vegetation, fire spread and fire behaviour on biomass burning and trace gas
14 emissions: results from a process-based model, *Biogeosciences*, 7(6), 1991–2011, 2010.
- 15 Timmermann, A., Oberhuber, J., Bacher, A., Esch, M., Latif, M. and Roeckner, E.: Increased El
16 Niño frequency in a climate model forced by future greenhouse warming, *Nature*, 398(6729),
17 694–697, doi:10.1038/19505, 1999.
- 18 Tosca, M. G., Randerson, J. T., Zender, C. S., Flanner, M. G. and Rasch, P. J.: Do biomass
19 burning aerosols intensify drought in equatorial Asia during El Niño?, *Atmos. Chem. Phys.*, 10(8),
20 3515–3528, doi:10.5194/acp-10-3515-2010, 2010.
- 21 Turetsky, M. R., Kane, E. S., Harden, J. W., Ottmar, R. D., Manies, K. L., Hoy, E. and Kasischke,
22 E. S.: Recent acceleration of biomass burning and carbon losses in Alaskan forests and peatlands,
23 *Nature Geosci*, 4(1), 27–31, doi:10.1038/ngeo1027, 2011.
- 24 Ward, D. S., Kloster, S., Mahowald, N. M., Rogers, B. M., Randerson, J. T. and Hess, P. G.: The
25 changing radiative forcing of fires: global model estimates for past, present and future, *Atmos.*
26 *Chem. Phys.*, 12(22), 10857–10886, doi:10.5194/acp-12-10857-2012, 2012.
- 27 Van der Werf, G. R., Dempewolf, J., Trigg, S. N., Randerson, J. T., Kasibhatla, P. S., Giglio, L.,
28 Murdiyarso, D., Peters, W., Morton, D. C., Collatz, G. J., Dolman, A. J. and DeFries, R. S.:
29 Climate regulation of fire emissions and deforestation in equatorial Asia, *Proc. Natl. Acad. Sci.*
30 *U.S.A.*, 105(51), 20350–20355, doi:10.1073/pnas.0803375105, 2008.
- 31 Van der Werf, G. R., Morton, D. C., DeFries, R. S., Olivier, J. G. J., Kasibhatla, P. S., Jackson, R.
32 B., Collatz, G. J. and Randerson, J. T.: CO₂ emissions from forest loss, *Nature Geosci*, 2(11),
33 737–738, doi:10.1038/ngeo671, 2009.
- 34 Van der Werf, G. R., Randerson, J. T., Collatz, G. J., Giglio, L., Kasibhatla, P. S., Arellano, A. F.,
35 Olsen, S. C. and Kasischke, E. S.: Continental-Scale Partitioning of Fire Emissions During the
36 1997 to 2001 El Niño/La Niña Period, *Science*, 303(5654), 73–76, doi:10.1126/science.1090753,
37 2004.
- 38 Van der Werf, G. R., Randerson, J. T., Giglio, L., Collatz, G. J., Kasibhatla, P. S. and Arellano Jr.,
39 A. F.: Interannual variability in global biomass burning emissions from 1997 to 2004, *Atmos.*
40 *Chem. Phys.*, 6(11), 3423–3441, 2006.
- 41 Van der Werf, G. R., Randerson, J. T., Giglio, L., Collatz, G. J., Mu, M., Kasibhatla, P. S.,
42 Morton, D. C., DeFries, R. S., Jin, Y. and van Leeuwen, T. T.: Global fire emissions and the
43 contribution of deforestation, savanna, forest, agricultural, and peat fires (1997–2009), *Atmos.*
44 *Chem. Phys.*, 10(23), 11707–11735, doi:10.5194/acp-10-11707-2010, 2010.

- 1 Venevsky, S., Thonicke, K., Sitch, S., and Cramer, W.: Simulating fire regimes in human-
2 dominated ecosystems: Iberian Peninsula case study, *Glob. Change Biol.*, 8, 984–998,
3 doi:10.1046/j.1365-2486.2002.00528.x, 2002.
- 4 Westerling, A. L., Turner, M. G., Smithwick, E. A. H., Romme, W. H. and Ryan, M. G.:
5 Continued warming could transform Greater Yellowstone fire regimes by mid-21st century, *Proc.*
6 *Natl. Acad. Sci. U.S.A.*, 201110199, doi:10.1073/pnas.1110199108, 2011.
- 7 Wilson, R. A. J.: A reexamination of fire spread in free-burning porous fuel beds [Wildland fuels,
8 forest fire management, model], USDA Forest Service Research Paper INT (USA), available at:
9 <http://agris.fao.org/agris-search/search.do?f=1983/US/US83048.xml;US8236661> (last access; 15
10 February 2014), 1982.
- 11 Wirth, C.: Fire Regime and Tree Diversity in Boreal Forests: Implications for the Carbon Cycle,
12 in *Forest Diversity and Function*, edited by D. M. Scherer-Lorenzen, P. D. C. Körner, and P. D.
13 E.-D. Schulze, pp. 309–344, Springer Berlin Heidelberg. [online] Available from:
14 http://link.springer.com/chapter/10.1007/3-540-26599-6_15 (Accessed 17 November 2014), 2005.
- 15 Yue, C., Ciais, P., Cadule, P., Thonicke, K., Archibald, S., Poulter, B., Hao, W. M., Hantson, S.,
16 Mouillot, F., Friedlingstein, P., Maignan, F., and Viovy, N.: Modelling fires in the terrestrial
17 carbon balance by incorporating SPITFIRE into the global vegetation model ORCHIDEE – Part 1:
18 Simulating historical global burned area and fire regime, *Geosci. Model Dev. Discuss.*, 7, 2377-
19 2427, doi:10.5194/gmdd-7-2377-2014, 2014.
- 20 Zhao, M. and Running, S. W.: Drought-Induced Reduction in Global Terrestrial Net Primary
21 Production from 2000 Through 2009, *Science*, 329(5994), 940–943,
22 doi:10.1126/science.1192666, 2010.

23

24

1 **Tables and figures**

2 Table 1 Comparison of simulated and GFED3.1 fire carbon emissions, burned area and total fuel
 3 consumption (TFC, including consumption of surface dead litter or organic soil, and live biomass)
 4 for different regions averaged over 1997–2009. The locations of the GFED regions are mapped in
 5 Fig. S5, the abbreviations expanded in the caption to Fig. 4. The last three columns provide a
 6 qualitative indication of the error in simulated carbon emissions and its attribution to those of
 7 burned area and TFC. To obtain the qualitative error information, the ratio of simulated value to
 8 GFED3.1 is compared to the coefficient of variation (CV) of the corresponding GFED3.1 value as
 9 following:

- 10 = , no error, if the ratio is within (1-CV, 1+CV);
 11 +, overestimated, if the ratio falls in (1+CV, 3);
 12 ++, moderately overestimated, if the ratio falls in (3,10);
 13 +++, highly overestimated, if the ratio is bigger than 10;
 14 -, underestimated, if the ratio falls in (0.3, 1-CV);
 15 --, moderately underestimated, if the ratio falls in (0.1, 0.3)

16 The CV for annual emissions and burned area by GFED3.1 data was calculated using the annual
 17 time series. Total fuel consumption data for GFED3.1 were obtained from Table 4 of van der Werf
 18 et al. (2010) and an arbitrary CV of 0.3 was adopted.

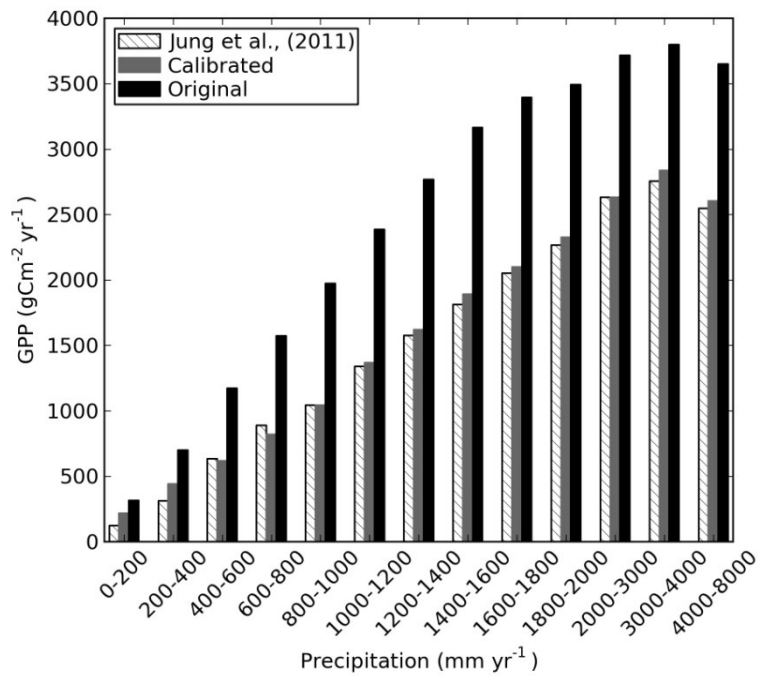
19

Region	Emissions (Tg C yr ⁻¹)		Burned area (Mha yr ⁻¹)		Total fuel consumption (g C m ⁻² of BA)		Emission error	BA error	TFC error
	GFED3.1	ORC	GFED3.1	ORC	GFED3.1	ORC			
BONA	54	45	2.1	3.3	2662	1385	=	=	-
TENA	9	96	1.5	18.5	627	514	+++	+++	=
CEAM	20	29	1.4	4.1	1489	714	=	+	-
NHSA	22	79	2.1	5.8	1007	1351	++	+	+
SHSA	272	369	20	35.7	1311	1035	=	+	=
EURO	4	13	0.7	1.5	667	874	++	+	+
MIDE	2	24	0.9	8.8	198	278	+++	+++	+
NHAF	480	680	129	58.7	377	1159	+	-	++
SHAF	556	331	125	34.1	448	969	-	--	+

BOAS	128	61	6.6	3.9	1979	1589	-	-	=
SEAS	103	40	14	4.1	253	969	-	-	++
CEAS	35	161	7	41.4	1459	388	++	++	--
EQAS	181	2	1.8	0.1	9500	1559	--	--	--
AUST	133	174	52	15.6	259	1118	=	-	++
Global*	1999	2104	364	236	549	891	=	-	+

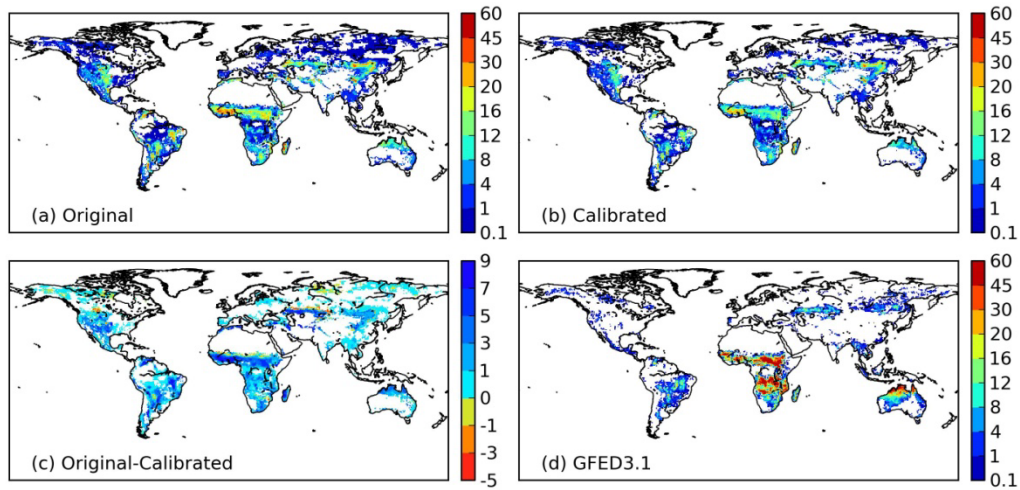
1
2
3
4

* For GFED3.1 data, burned area and emissions from all types of fires are included, i.e., forest fire, grassland fire, woodland fire, agricultural fire, deforestation and peatland fire.

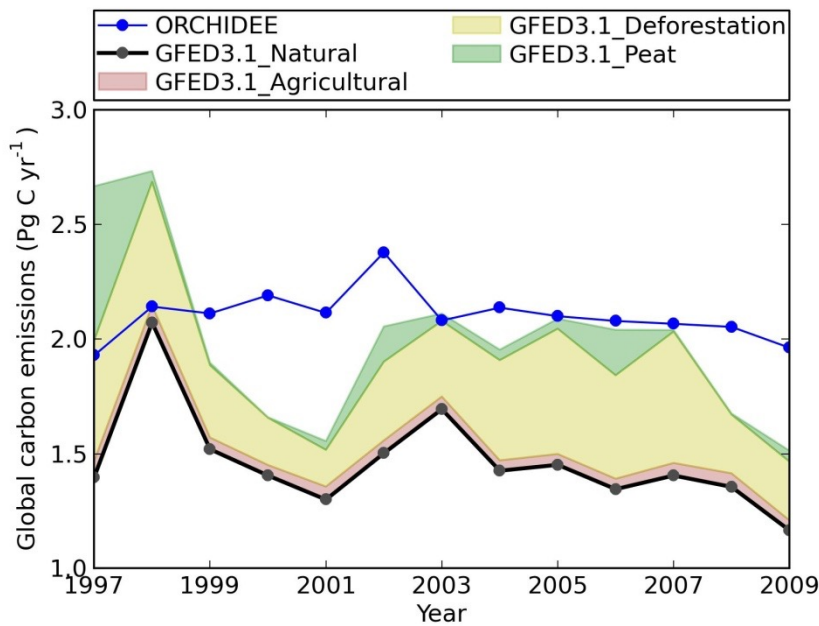


5
6
7
8

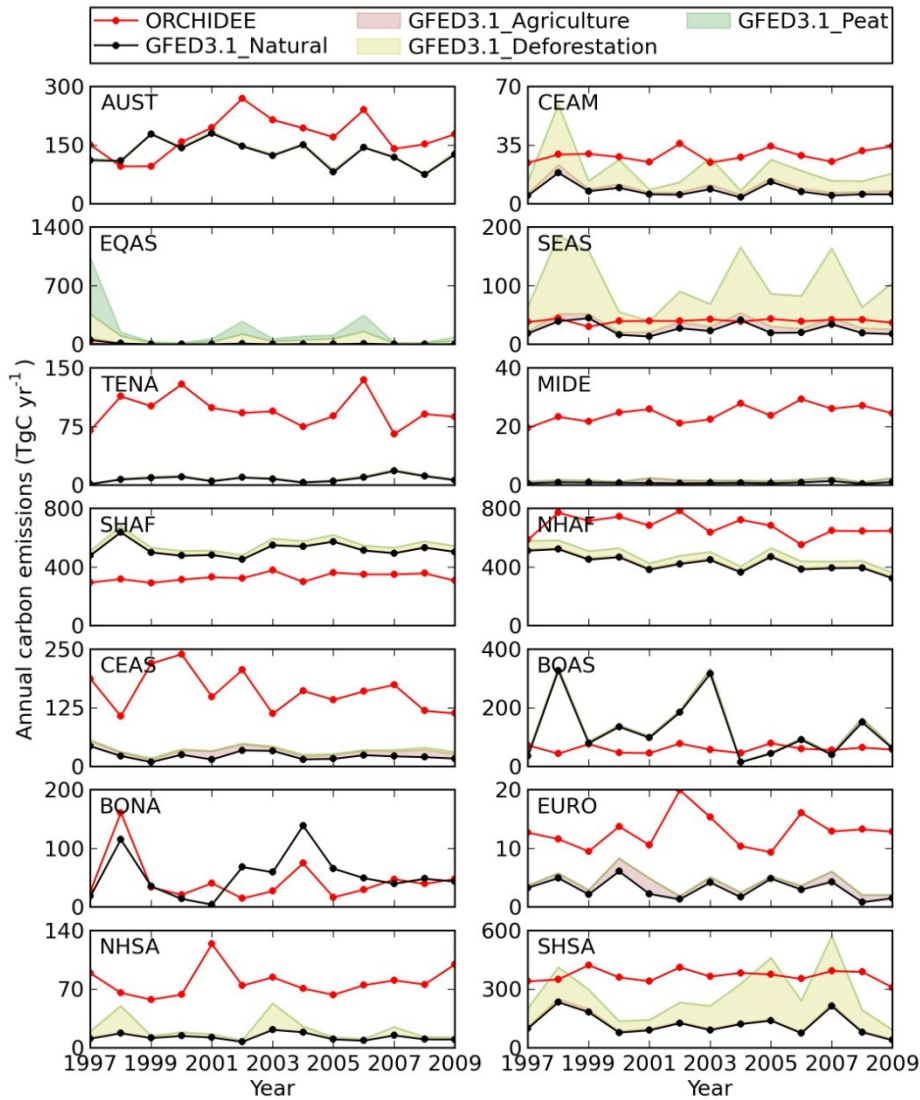
Fig. 1 Annual GPP as a function of annual precipitation according to Jung et al. (2011) (dashed bar), model simulation before (black bar) and after calibration (grey bar).



1
 2 Fig. 2 Simulated mean annual burned fraction (%) for 1997–2009 for (a) original and (b)
 3 calibrated model productivity. The change in burned fraction (original - calibrated) is shown in
 4 panel (c), and the burned fraction by GFED3.1 data is shown in panel (d).
 5

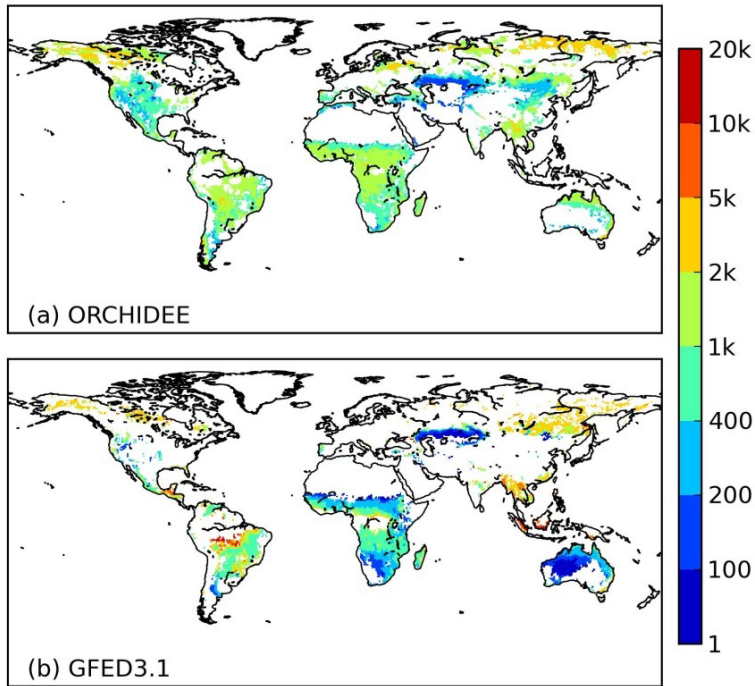


6
 7 Fig. 3 Annual global fire carbon emissions for 1997–2009 simulated by ORCHIDEE (blue), and
 8 from the GFED3.1 data. Carbon emissions from natural sources (forest fire, grassland fire, and
 9 woodland fire) are shown as the black solid line. Carbon emissions from agricultural fire,
 10 deforestation fire and peat fire (which are not explicitly simulated in ORCHIDEE) are shown as
 11 shaded areas stacked on top of GFED3.1 natural source fire carbon emissions.

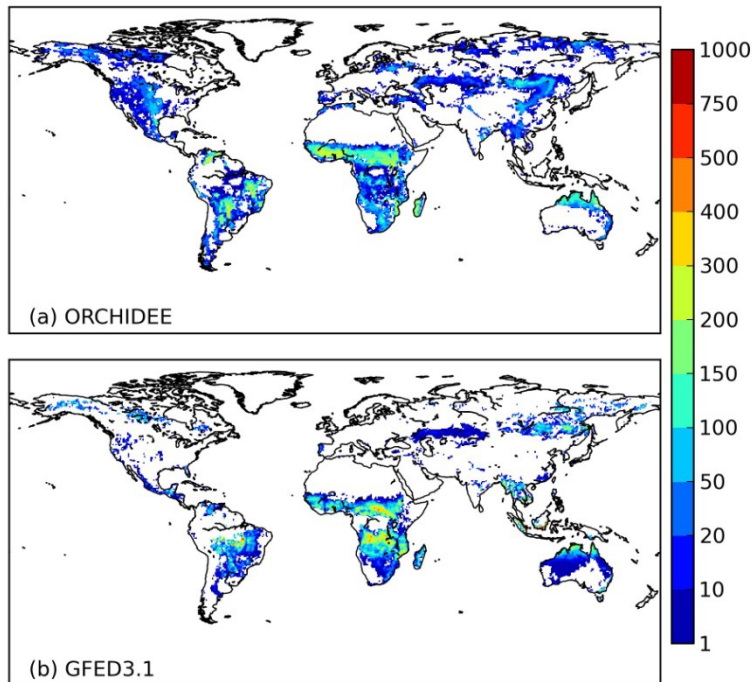


1

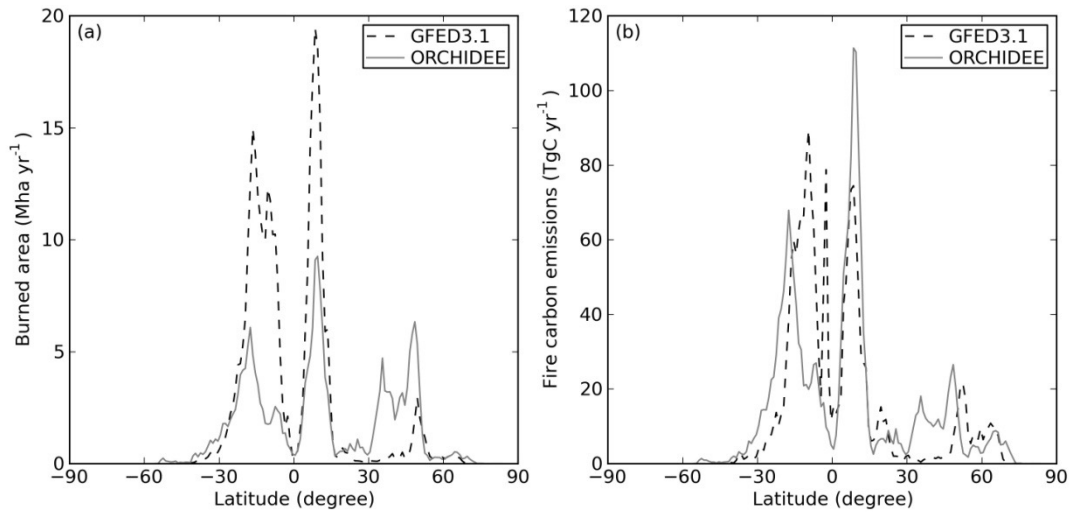
2 Fig. 4 Annual fire carbon emissions simulated by ORCHIDEE and from the GFED3.1 data for
 3 1997–2009 for the 14 different GFED regions. The 14 GFED regions are, BONA: Boreal North
 4 America; TENA: Temperate North America; CEAM: Central America; NHSA: Northern
 5 Hemisphere South America; SHSA: Southern Hemisphere South America; EURO: Europe;
 6 MIDE: Middle East; NHAF: Northern Hemisphere Africa; SHAF: Southern Hemisphere Africa;
 7 BOAS: Boreal Asia; CEAS: Central Asia; SEAS: Southeast Asia; EQAS: Equatorial Asia; AUST:
 8 Australia and New Zealand. Refer to Fig. S5 for their distributions.



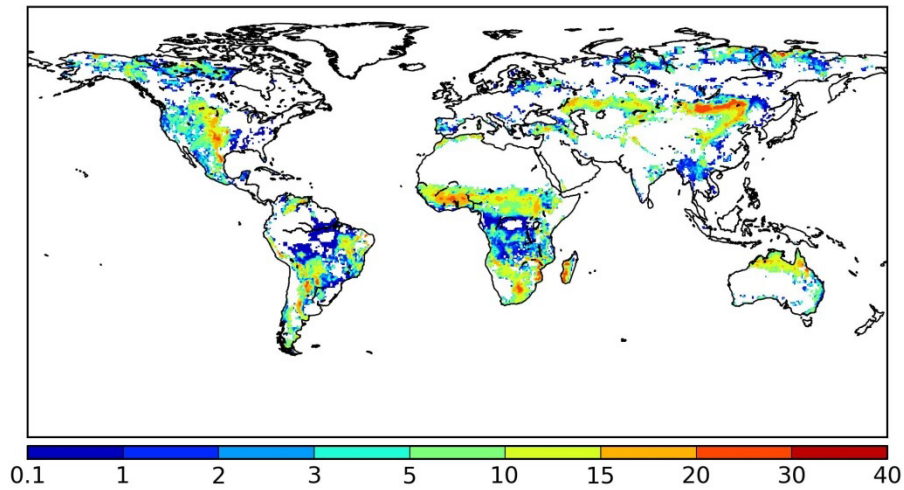
1
 2 Fig. 5 Fuel consumption (g C per m^2 of area burned) averaged over 1997–2009 by (a) ORCHIDEE
 3 simulation and (b) the GFED3.1 data.



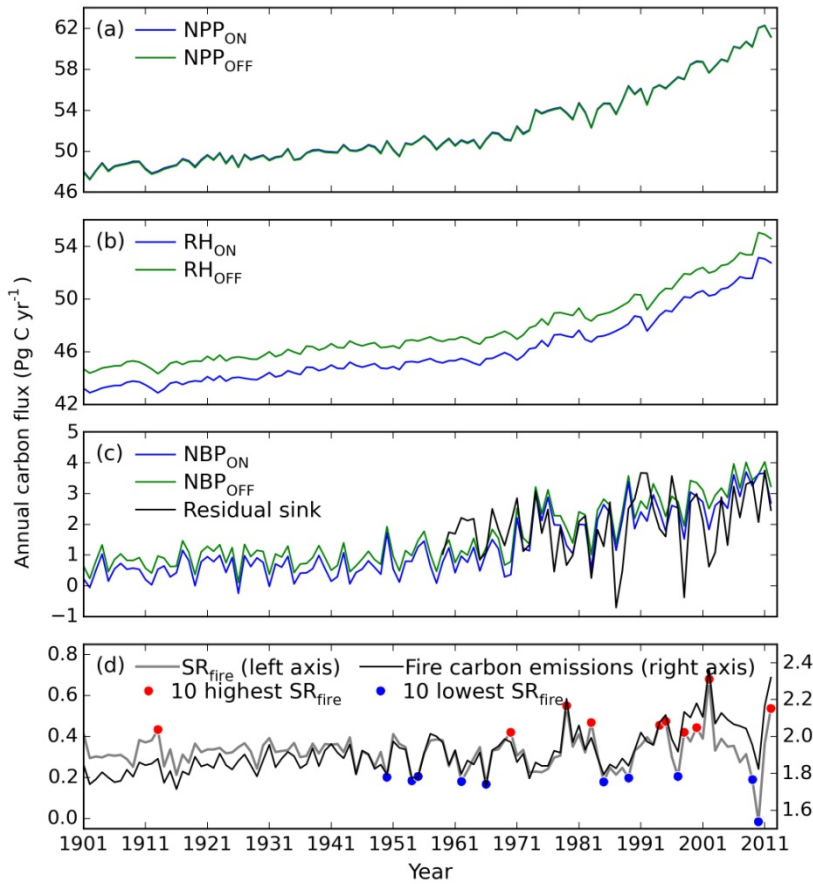
4
 5 Fig. 6 Mean annual carbon emissions (g C m^{-2}) for 1997–2009 by (a) ORCHIDEE simulation and
 6 (b) the GFED3.1 data, based on the whole grid cell area included both burned and unburned parts.



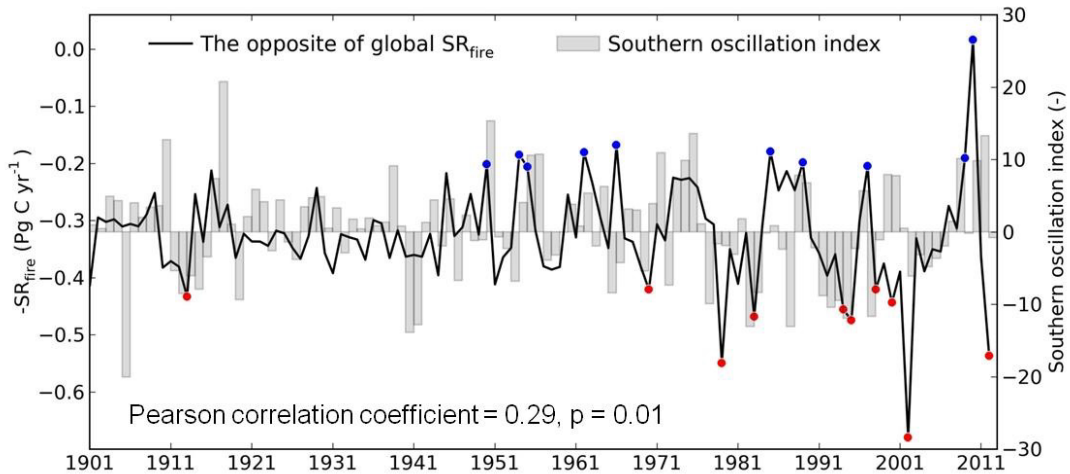
1
 2 Fig. 7 The latitudinal distribution of (a) burned area and (b) fire carbon emissions as simulated by
 3 ORCHIDEE (grey solid line) and by the GFED3.1 data (black dashed line).



4
 5 Fig. 8 The fire carbon emissions as percentage (%) of net primary production (NPP) for 2003–
 6 2012.
 7



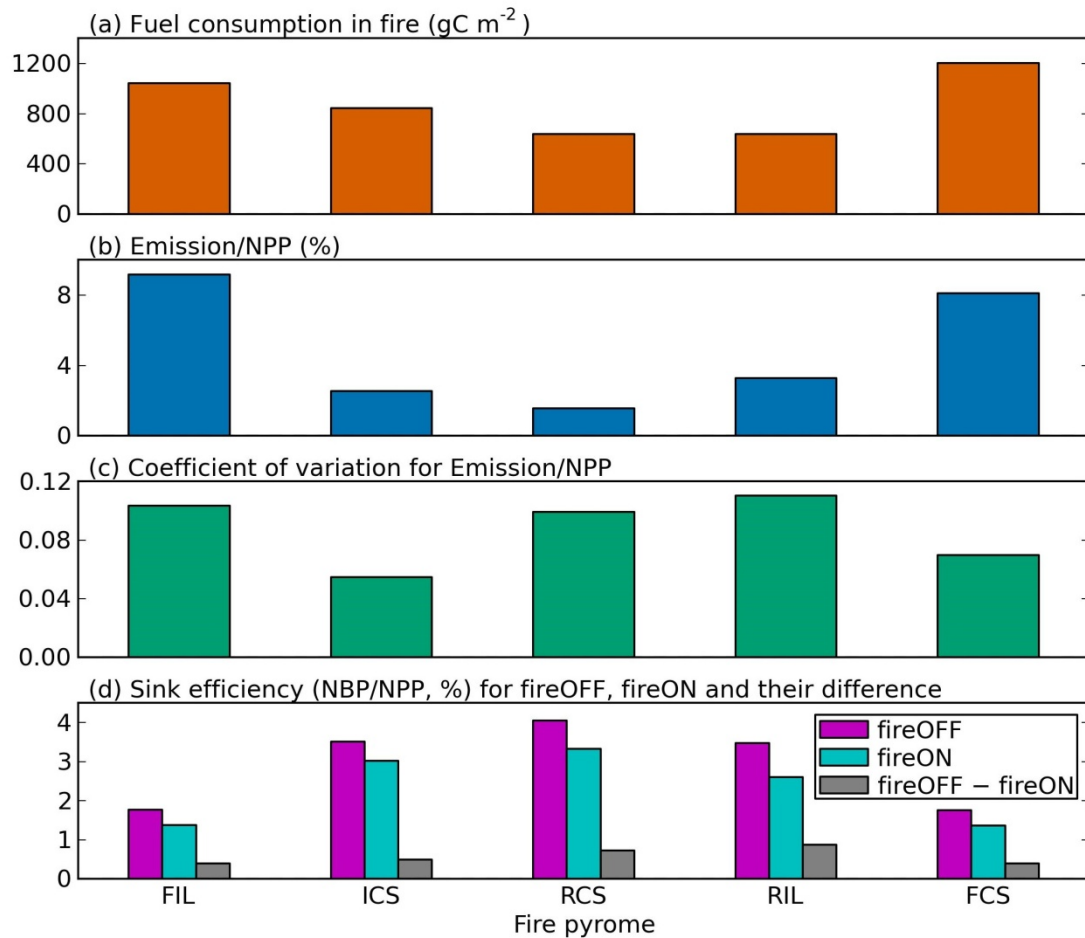
1
 2 Fig. 9 Different components of global carbon fluxes for fireON and fireOFF simulations. The
 3 carbon fluxes are (a) NPP; (b) heterotrophic respiration (RH); (c) NBP and the residual land sink
 4 as reported by Le Quéré et al. (2013); and (d) The NBP reduction by fires ($SR_{fire} = NBP_{OFF} -$
 5 NBP_{ON} , in grey, left vertical axis) and fire carbon emissions (black, right vertical axis).



6
 7 Fig. 10 The fire-induced sink reduction (left vertical axis, $-SR_{fire}$) and its correlation with the
 8 Southern Oscillation Index (SOI, right vertical axis) which is an indicator for the El Niño
 9 Southern Oscillation (ENSO) climate oscillation. The red dots indicate the ten highest SR_{fire} years
 10 and the blue dots indicate the ten lowest SR_{fire} years. Note that the left vertical axis shows the

1 opposite of SR_{fire} .

2



3

4 Fig. 11 Characteristics of different fire pyromes (defined as by Archibald et al., 2013) in terms of
5 the role of fires in the terrestrial carbon balance. (a) Fuel consumption in fire; (b) Emissions as
6 percentage of NPP; (c) Coefficient of variation for the ratio of emissions against NPP; and (d)
7 Sink efficiencies (i.e., NBP/NPP) for fireOFF and fireON simulations and their difference. All
8 variables are shown for 1901–2012 except the fuel carbon consumption which is averaged over
9 2003–2012. The five fire pyromes are: FIL, Frequent–Intense–Large; ICS, Intermediate–Cool–
10 Small; RCS, Rare–Cool–Small; RIL, Rare–Intense–Large; FCS, Frequent–Cool–Small. Refer to
11 Fig. S2 for their spatial distributions.